Final report

to the

National Aeronautics and Space Administration

On Research Supporting

Experimental and Analytical Studies for a Computational Materials Program

NAG 1-1780

W.G. Knauss

California Institute of Technology
Pasadena, California 91125

August 1999

The studies supported by Grant NAG 1-1780 were directed at providing physical data on polymer behavior that would form the basis for computationally modeling these types of materials.

Because of ongoing work in polymer characterization this grant supported part of a larger picture in this regard. Efforts went into two combined areas of their time dependent mechanical response characteristics: Creep properties on the one hand, subject to different volumetric changes (nonlinearly viscoelastic behavior) and time or frequency dependence of dilatational material behavior.

The details of these endeavors are outlined sufficiently in the two appended publications, so that no further description of the effort is necessary.

Attachments:

1. The Temperature and Frequency Dependence of the Bulk Compliance of Poly(Vinyl Acetate). A Re-Examination. T.H. Deng and W.G. Knauss. *Mech. Time Dep. Mat.* **1** 33-49. 1997

2. The Role of Dilatation in the Nonlinearly Viscoelastic Behavior of PMMA under Multiaxial Stress States, by H. Lu and W.G. Knauss
   To appear this year in the journal of *Mechanics of Time Dependent Materials.*

Mechanics of Time Dependent Materials

The Role of Dilatation in the Nonlinearly Viscoelastic Behavior of PMMA under Multiaxial Stress States

H. Lu

Graduate Aeronautical Laboratories, California Institute of Technology, Pasadena, California 91125–
Now Assistant Professor of Mechanical and Aerospace Engineering at Oklahoma State University, Stillwater, Oklahoma 74078, USA

W.G. Knauss
Professor of Aeronautics and Applied Mechanics, *Graduate Aeronautical Laboratories, California Institute of Technology, Pasadena, California 91125, USA*

(Received and accepted December 1998)

Abstract. In order to better understand phenomena related to "yield-like" behavior of polymers, the nonlinear thermo-mechanical behavior of Polymethyl Methacrylate (PMMA) under combined axial (tension, compression) and shear stress states (torsion) is investigated on thin walled cylindrical specimens at temperatures between $22°C$ and $110°C$. In contrast to the mutual independence of shear and dilatational response under conditions appropriate for linearized viscoelasticity, one observes an increasingly strong influence of the first stress or strain invariant on shear creep at shear strains in excess of 0.5%. While shear stresses alone elicit nonlinear response in creep (rates) as "intrinsically nonlinear shear response", the superposition of small positive dilatation accelerates

shear deformations while negative dilatation retards it in qualitative agreement with free volume arguments when comparison is effected via maximum shear. In addition, an isochronal representation of the "intrinsically nonlinear shear response" demonstrates that the nonlinear behavior becomes more pronounced the closer one approaches the glass transition temperature from below.

Keywords: Nonlinear viscoelasticity; polymer yielding; free volume; multiaxial creep; time dependent properties.

1 Introduction

In spite of the tremendous increase in polymer applications to engineering problems there exists a surprising lack of knowledge regarding polymer nonlinear behavior at elevated load or deformation levels. To date, simple shear or uniaxial stress fields serve almost exclusively to characterize the mechanical properties of these materials. Such a simplistic approach to material characterization is clearly inadequate when large strains and high stresses are involved that can and will lead to failure/fracture. For example, crack propagation is an important aspect of evaluating the strength and life expectancy of polymeric structures. While linearly viscoelastic crack propagation models exist (Müller and Knauss, 1971; Knauss, 1974; Schapery, 1975) which correspond roughly to the Griffith model for rate independent, brittle fracture, their extension to nonlinearly viscoelastic material behavior is not thoroughly investigated because the nonlinearly viscoelastic description of the material constitution for arbitrary (uniaxial and multiaxial) loading histories and environmental (temperature, moisture content, etc.) conditions is not available. It is thus not possible to expand the investigation of linearly viscoelastic fracture models to nonlinear material behavior, similar to how plasticity considerations have extended the application of linear fracture mechanics to the engineering metals, until the nonlinear, time dependent behavior of these materials is understood more completely.

While there exist numerous investigations on the nonlinear time dependent behavior in one dimensional stress or strain states, (sometimes superposed on pressure), investigations on the nonlinear viscoelastic behavior under multiaxial stress or strain states are sparse. Most are restricted to the formulation of yield or flow rules along plasticity lines, (Thorkildsen, 1964; Sternstein and Ongchin, 1969; Carapellucci and Yee, 1986), so that the time dependent characteristics are not considered. For example, Sternstein and Ongchin (1969) showed that the craze instability, considered as a "yield phenomenon", depended linearly on pressure. We take the view here that the yield-like responses of polymers observed in the uniaxial stress state are a direct consequence of the evolutionary character of the constitutive response rather than only a distinct physical process similar to the classical metal yield. While classical yield behavior is typically associated with equivoluminal deformation behavior, we shall see that this latter characteristic of metals does not apply to polymers (at least not to PMMA), so that the common term of "yielding" may not really be appropriate. To express this difference we adhere here to the term "nonlinear viscoelasticity" or "yield-like" behavior.

Underling the subsequent developments is the understanding that when polymers undergo other than infinitesimal deformations, these are predominantly due to the shear com-

ponent(s), the dilatational component being typically very small in comparison, except when extremely high pressures are involved. For this reason it seems mandatory to be concerned with the shear behavior in describing the nonlinear mechanical constitution of polymers rather than the uniaxial response so predominantly employed in current investigations of nonlinear response of polymers. While this understanding is almost intrinsically understood in connection with nonlinear deformations in metals, it is only sparsely recognized (see e.g. Lee and McKenna, 1990) in the more recent polymer mechanics literature.

Thus, very few results are reported on time dependent polymer behavior under multiaxial loading. Ewing, *et. al.* (1972, 1973) investigated the creep behavior of Polyethylene and found that under combined tension and torsion the equivalent stress is related isochronically to the equivalent strain by a power law under moderate strains, provided the material is considered incompressible (Poisson ratio = 0.5). McKenna and co-workers have investigated the interaction between torsion and axial forces or dilatation in several studies. While the normal-force/torsion relation has been documented by McKenna and Zapas (1979, 80) for PMMA and (diluted) (Poly)Isobutylene, Duran and McKenna (1990) investigated explicitly the torsional relaxation behavior of Epoxy glass cylinders under constant length constraint at room temperature, while simultaneously and carefully measuring the resulting axial force and dilatation as a function of time. While we shall later see that dilatation affects the time dependence of the shear response (torsion) at moderate strains, the Duran and McKenna data imply that the converse also holds.

Starting with the observation that such very small volume changes as are associated with temperature (Williams *et.. al.* 1955), moisture (Knauss and Kenner, 1980) and pressure (Fillers and Tschoegl, 1977; Moonan and Tschoegl, 1983, 84, 85) can have remarkably strong effects on the relaxation or retardation times, Knauss and Emri (1981, 87), and Losi and Knauss (1992) explored the formulation of "free volume" clock models for describing nonlinearly viscoelastic behavior. More recently, McKenna (and co-workers) has questioned the appropriateness of a volume-clock based on measurements performed on an Epoxy glass (Santore, Duran and McKenna, 1991; McKenna, 1994). The Knauss and Emri (1981, 87), and Losi and Knauss (1992) models included linearly viscoelastic behavior as a natural limit case for small strains and provided surprisingly close simulation for responses in one dimensional stress states for deformations in the 1 to 10% strain range. However, this formulation circumvented the question of nonlinear behavior under purely shear deformations when volumetric effects should be minimized. As a consequence, we study here the interaction of volumetric and shear deformation and to what extent it influences or controls nonlinearly viscoelastic response.

In the sequel we consider first the experimental aspects followed by the measurement

results and analysis in section 3. Conclusions are summarized in section 4.

2 Experimental Aspects

This section describes the specimen preparation, its geometry, experimental setup, and measurement methods. We start with the

2.1 Specimen Geometry and Preparation: The material is commercially cast PMMA stock, 38 mm in diameter (ACE, now a part of Ono, $T_g = 105°C$)[1]. Cast instead of extruded rods were chosen to avoid possible anisotropy due to molecular alignment incurred during processing. Each rod, delivered in 152 cm lengths was cut into blanks roughly one cm longer than the finished specimen length and the short rods were annealed in the Texaco ISO 46 hydraulic oil (boiling point= $355°C$) at $115°C$ for four hours and then cooled to room temperature slowly by interrupting the power to the temperature chamber, resulting in a cooling rate of about $5°C/hr$. This annealing process was necessary to remove the memory of thermal and loading history stored in the material during the casting process[2].

Employing oil as an environmental medium raised the issue of whether this preparation step influenced the conclusions reached in this study in a significant way. The answer to this question is "no". Since all specimens were annealed by the identical process, one would have to argue that all specimens were identical in this sense. Thus the only question remains whether the specimens were changed significantly in the annealing process, if that were important. To estimate that possibility, specimens were weighted before and after the annealing process, and were found to have increased their weight by less than 0.002%. Upon translating this change via a free-volume argument into a change of the glass transition temperature, one would find a roughly $1°C$ decrease in its value.

During the machining process, coolant was constantly circulated in order to avoid excessive heating. The finished specimens, illustrated in figure 1, were annealed again in the hydraulic oil bath at $115°C$ for 4 hours to remove any residual surface stress developed during machining.

In order to minimize specimen-to-specimen variations they were re-used as much as possible. This required reconditioning through heating the specimens in order to remove

[1] Although a seemingly large volume of material was acquired initially for this study, a re-order produced a material of clearly different properties; the company had changed ownership again. As a result, additional data desired for further evaluation in this study could not be obtained any more.

[2] It was found that if the rod was not annealed before machining, the specimen would deform upon annealing subsequent to the machining.

previously incurred deformations. Care was thus necessary to minimize the effect of physical aging (Struik, 1978, Lee and McKenna, 1990, Brinson and Gates, 1996). A separate study determined that aging specimens at least 48 hours at $22°C$ was sufficient for the duration of the measurements described later on. As an example we show in figure 2 that at two select temperatures the shear creep behavior of specimens aged longer than two days exhibit no aging effect within the test period of $10^4 s$. Typically, aging times were somewhat longer than two days (usually longer than $2 \times 10^5 s$) and shorter than two weeks.

Two kinds of thin-walled specimens were used. The first possessed an outer diameter of 22.23 mm, a wall thickness of 1.59 mm and a test length of 88.9 mm. The ratio of the wall thickness to the radius was thus 0.14. A thinner wall is not practical because torsion induced buckling may occur at the strain levels used. Based on an elastic buckling analysis, these specimens can reach a maximum surface shear strain in the range of $4.0 - 4.5\%$ before buckling when an estimation of the Poisson's ratio in the range of $0.33 - 0.4$ is used[3]. In order to increase the permissible shear strain, specimens with a thicker wall were also used for temperatures near the glass transition. The thicker specimens possessed an outer diameter of 25.15 mm, a thickness of 3.18 mm and a test length of 76.2 mm. The ratio of the wall thickness to the radius was then 0.29, which allowed achieving a maximum surface shear strain in the range of $8.5 - 12.5\%$ before (elastic) buckling when an estimation of a poisson's ratio in the range of $0.33 - 0.45$ is used. The actual maximum shear strain in the experiment could be slightly different from these estimations based on elastic buckling analysis since viscoelastic effects were involved. The geometry of the specimen was monitored continuously through the non-contact strain measurement method identified below to sense the possible onset of buckling and all data were thus acquired without interference by buckling; no buckling was ever observed.

The moisture content in amorphous polymers can have a significant effect on viscoelastic behavior (Knauss and Kenner, 1980). The volumetric dilatation due to moisture content has the same effect on the creep behavior as temperature if the induced volumetric deformations are the same. To minimize this, the specimens were stored and used at the same relative humidity at all times. An environment of 6% of relative humidity at room temperature was produced (Lide, 1995) via a saturated sodium hydroxide solution within an enclosed bell-jar in which the annealed PMMA specimens were stored for at least two weeks prior to use. The weight of each specimen was measured every few days and found to decrease initially but to remain constant after three days (Mettler electronic balance, model HL 32 with an accuracy of 0.1 mg). The 6% relative humidity level could not be maintained in the test

[3]If the buckling instability is expressed in terms of an applied torsional strain, the modulus does not enter the estimate, but only Poisson's ratio ν. The torsional strain at buckling is proportional to $(1+\nu)(1-\nu^2)^{-3/4}$.

chamber (a custom designed Russel's chamber) at all temperatures; instead the humidity levels were always kept as low as possible, which occurred according to the data in Table 1.

Table 1: Relative humidity at test temperatures

Temp.$^\circ C$	22	35	50	65	80	90	100	110
%R.H.	25.7	15.2	6	6	1.8	1.7	1.6	1
Error	± 3	± 3	± 2	± 1	± 0.2	± 0.2	± 0.2	± 0.2

2.2 Loading history: We employ creep experiments under proportional loading, characterized by simultaneous axial and torsion loading. These loads were applied in an MTS system within a second, and the resulting deformation was analyzed (see below) for times greater than ten seconds, to allow loading transients to die out, as estimated on the basis of linear viscoelasticity[4]. The hydraulic MTS 809 system has the dual capacity of 15 kN of axial force and 168 $N \cdot m$ of torque, the measurement resolution being $\pm 0.5N$ and $\pm 0.08N \cdot m$, respectively.

Data is typically presented in the form of a "creep compliance": The shear compliance $J(t)$ is given by the engineering shear strain $2\epsilon_{x\theta}(t)$ divided by the applied corresponding shear stress τ(=const.)[5], and the uniaxial compliance D(t) by the axial strain $\epsilon_{xx}(t)$ normalized by the axial stress σ(=const.). The strain distribution across the wall thickness was assumed to be linear on the basis of simple kinematics considerations. However, the corresponding distribution of shear stress τ is then only approximately linear across the cylinder wall. Using linear estimates the variation of stress from the average was $\pm 7\%$ for the thinner walled cylinders and $\pm 14.5\%$ for the other one; for typically nonlinear behavior these estimates are upper bounds. The stresses entering the compliances are the values on the cylinder surface.

Tests were conducted at a constant temperature and at humidity levels indicated in table 1. the temperature was monitored continuously by a thermocouple near the specimen to within $\pm 0.2^\circ C$. The specimen, gripped by a well aligned fixture[6] (Lu, 1997), was illuminated

[4]Based on the paper by Zapas, McKenna, and Brenna (1989), which deals with the time dependence of a nonlinearly viscoelastic liquid, McKenna has suggested that this time characterizing loading transient can be significantly reduced (McKenna, 1999)

[5]In linear viscoelsticity the creep compliance, the ratio of the measured (time-varying) shear strain to the (constant) applied shear stress, is a material property since it is a material function representing the time dependent behavior of the material. In nonlinear behavior this stress and strain proportionality is no longer valid, so that the "creep compliances" measured here are, strictly speaking, functions of the deformations also. We adhere to the use of this ratio and to the nomenclature out of convenience.

[6]The authors are indebted to Dr. T. Nicholas of the Wright Laboratories for providing the basic design.

with two Halogen lights (Fuji, $12V$, $20w$) outside of the chamber so that heating of the specimen was not an issue.

2.3 Strain measurement method: The specimens (*c.f.* figure 1) were used over a wide range of temperatures, including those near the glass transition where polymers become very "soft". Under such conditions strain gauges cannot be used. The method of computing deformations from the end displacements and rotation angles may not be accurate when the possibility of inhomogeneous deformations exist. Therefore, a non-contact measurement technique based on digital image correlation (Sutton, *et. al.* 1983) and tailored to measurements on cylindrical specimens (Lu, Vendroux and Knauss, 1997) was used.

3 Results

In the sequel we report shear creep measurements (torsion) with and without superposed axial loads (dilatation) at different temperatures. Consideration is given first to pure shear loading, followed by a demonstration that the presence of a positive or negative first stress (strain) invariant causes, respectively, acceleration or retardation in the creep response.

3.1 Pure shear response: Figures 3-6 present the shear creep responses derived from purely torsional loads at various temperatures. There is a clear dependence of the strain response on the load level, higher load levels leading to faster creep at all temperatures. The most complete data set available is that obtained at $80°C$ which becomes the primary basis of the analysis. The data at other temperatures is then examined for the same systematic behavior. To the extent possible or necessary we show also data derived from small strain relaxation tests (Lu, Zhang and Knauss, 1997) by inversion of the appropriate convolution integral, which is then identified as linearly viscoelstic behavior. In particular, note that at $22°C$ the creep compliance in shear derived from a 14.4 MPa load coincides with the small strain relaxation (inverted) data, so that this range can be reasonably identified as belonging to the linearly viscoelastic range. By contrast, when the shear stress increases to 29.2 MPa, the shear creep behavior is accelerated relative to the small-strain shear creep compliance, indicating that the material exhibits now nonlinear behavior.

3.1.1 Isochronal representation: It is of interest to present the pure shear data isochronally: Starting with the data for $80°C$ we cross-plot the strain achieved under a given stress for a set of fixed times against the stress. A linearly viscoelastic solid would generate a fan of

straight lines emanating from the origin, with longer times producing lines of lower slope (lower "modulus"). The result for the $80°C$ data is shown in figure 7. Two features stand out: For stress or strain values above 7.6 MPa or 0.5% shear strain there exists a "fan" that centers at about these values. While at $80°C$ no detailed measurements were made at stress levels lower than this value, we assume for present analysis purposes that the material can be described as behaving in a (nearly) linearly viscoelastic manner. We shall refer to the fan center as the "yield region" or simply as the "yield point". Above this value creep rates are clearly accelerated. A detailed analysis shows that the data points do not fall precisely on straight lines as depicted, though it could be argued that the precision of the measurements makes it debatable whether this representation is allowed. It is advantageous, if only for illustrative purposes, however, to demonstrate the nonlinear behavior in this way. Other materials may require a different interpretation. The two traces below the "yield region" represent the shortest and longest times for linearly viscoelastic response covered in these tests.

This "bilinear" approximation may be represented by (ϵ_s =shear strain, τ= shear stress)

$$\begin{aligned} \epsilon_s &= J(t)\tau & \tau < \tau_0 \\ &= J(t)\tau + J_p(t)(\tau - \tau_0) & \tau \geq \tau_0 \end{aligned}$$

where the function $J_p(t)$ is shown in figure 8 represented by a power law over the stress range and time scale exhibited, namely

$$J_p(t) = J_{p0}t^{\alpha}, \qquad J_{p0} = 2.78 \times 10^{-4} MPa^{-1}, \ \alpha = 0.29.$$

Although the amount of creep data that could be obtained at other temperatures is less extensive it is instructive to represent those sets in a similar way, assuming a straight line representation for the nonlinear creep portion. Four sets of these data are shown in figure 9, again together with the $80°C$ data to ease comparison for later discussion. We draw on this representation later to estimate shear behavior in the nonlinear region in connection with effects of the first stress (strain) invariant(s) on the creep behavior.

To the extent that these data sets represent behavior similar to that observed at $80°C$, it is of interest to compare the values of the stresses or strains associated with the "yield regions" as a function of temperature: While the stress values show a monotonic decrease with temperature, the strains do so to a markedly lesser degree than the stresses. The data support thus a view of yield-like response that is characterized by achieving a critical strain rather than a critical stress. This critical strain is on the order of half a percent.

It is, perhaps, premature to ascribe any universal significance to this low value of strain for the onset of nonlinear behavior. Typically, values of one to two percent are quoted more

often, although in most of those cases the definition of "onset of nonlinearity" is defined poorly or at least differently. McKenna has observed divergent behavior, reporting deviation from linear shear stress-strain behavior of PMMA at about or above 1% strain (McKenna and Zapas,1979) while observing break down of the linear superposition principle at strains less than 0.5% (McKenna, G.B., NIST, unpublished work).

On the other hand, it is significant that the fans in figure 9 broaden systematically, as the temperature increases from 22 to 100°C, so that, qualitatively speaking, the nonlinearity of the material increases on approaching the glass transition temperature from below. The fan angle is determined by the function $J_p(t)$.[7]. As stated before, the number of data points that define the fans for temperatures other than 80°C are limited so that a definitive quantification of that trend may be, statistically speaking, not very precise. However, this trend is reflected in table 2 for the two characterizing parameters of the function $J_p(t)$, where the parameter α is seen to vary monotonically with the temperature. The value of J_{p0} appears to vary with temperature, but varies from a uniform value by less than the maximum possible error (a factor of two), which is the result of performing two curve-fits to the data for extracting this value.

Table 2: J_{p0} and α at four temperatures

Temp.°C	22	35	80	100
J_{p0} $(1/MPa)$	3.68×10^{-4}	4.21×10^{-4}	2.78×10^{-4}	5.68×10^{-4}
α	0.10	0.11	0.29	0.34

In the interest of comparing these values of shear-based yield with more conventionally defined interpretations (Bauwens-Crowet, 1973)[8] We draw on selected data for PMMA as supplied by Bauwens-Crowet (1973) and analyzed by Povolo and Hermida (1995). While we have no information on the similarities of or differences between the chemical constitution of the material represented in the Bauwens-Crowet data *vis-à-vis* the material used in our studies, such a comparison is nevertheless instructive, since differences in mechanical

[7]Whether this behavior may be captured through a time-temperature trade-off principle similar to that for linearly viscoelastic behavior needs to be investigated separately

[8]The subsequent data are taken from the paper by Povolio and Hermida (1995). It needs to be pointed out that the yield behavior as defined in this reference is not really a constitutive description. Rather, it represents an extremum in the uniaxial stress-train response under a specific deformation history. While this same limitation holds for the present description, the latter has, nevertheless, the possibility of defining the boundary between linear and nonlinear material representation, and is thus potentially part of a general constitutive description. A full constitutive description of nonlinear response under arbitrary deformation or stress histories is also not (yet) defined.

properties by factors of two or more are hardly expected. To compensate for the difference in stress states underlying the referenced data we represent the current shear data as equivalent uniaxial stresses. Figure 10 shows "yield behavior" at different temperatures as resulting from (a) uniaxial tension and (b) compression under uniform deformation rates, as well as (c) from shear creep according to figure 9. For the uniaxial data only two extreme deformation rates are represented in order to maintain the clarity of data representation. Several features stand out:

1. The "yield stress" resulting from tensile stresses is typically lower than that derived from compressive stress states. This behavior is consistent with the results developed in the present study, inasmuch as compressive stresses retard creep deformations and thus delay onset of nonlinear behavior; compressive stresses are equivalent to higher deformation rates.

2. For either tensile or compressive stresses, the lower rates of deformation exhibit lower values for the "yield stress" (slower rates or longer times lead to a lowering of the "yield response".

3. The "yield point" as defined through the isochronal shear response decreases also with increasing temperature, but less dramatically than the "uniaxial" data.

4. The "yield points" as defined through the shear response in figure 9 are typically lower than the values derived from the constant strain rate histories in uniaxial tension.

The reason for the observation under point 4 is, most likely, that the uniaxial data does not deal with the onset of nonlinear behavior, but with an extremum value in the stress-strain response that occurs at later values of higher stress and strain.

3.1.2 Examination of the stress clock phenomenon: Non-linearly viscoelastic deformation behavior has been formulated by various authors (Bernstein, Kearsly and Zapas (BKZ), 1963; Schapery, 1969; Hasan and Boyce, 1995; Lustig, Shay and Caruthers, 1996, Wineman and Waldron, 1995). While explaining all of these variations in the present context exceeds the scope of this presentation, we examine, in part as a consequence of personal discussions, the stress-clock framework (Schapery, 1969) formulated with the aid of irreversible thermodynamics. This model is often used for the one dimensional deformation in the form

$$\epsilon = g_0\mu_0\sigma + g_1\int_0^t \Delta\mu(\psi - \psi')\frac{dg_2\sigma}{d\tau}d\tau, \qquad (1)$$

where μ_0 and $\Delta\mu(\phi)$ are the initial and transient components of the linearly viscoelastic creep compliance $\mu(t)$, respectively. g_0, g_1, and g_2 are stress dependent material properties and

$$\psi = \psi(t) \equiv \int_0^\tau \frac{dt'}{a_\sigma}; \quad \psi' \equiv \psi(\tau) \equiv \int_0^t \frac{dt'}{a_\sigma}. \tag{2}$$

In general, a_0 may depend on both stress and/or strain, as discussed extensively by McKenna (1994) and by O'Connel and McKenna (1997) in connection with physical aging studies. However, it is often assumed to depend on stress only (Schapery, 1969; Lou and Schapery, 1971, Tervoort et al, 1996), so that there results a time-stress superposition process: The "transient" components of the creep compliance obtained at different stress levels is shifted (either horizontally or vertically, or both) to form a master curve. In the sequel we examine stress-governed time shifting along the logarithmic time axis, a process often associated with the notion of a "material stress clock".

It will be observed in figures 3 to 6 (temperatures of 22, 35, 80 and 100°C) that at short times the shear creep compliances at all stress levels are nearly the same; this observation is more pronounced at the lower temperatures[9]. This indicates that the nonlinearity evolves under load, but is suppressed early in the load history, when strains are still small.

As a result the creep curves present different slopes and curvatures, and their superposition by horizontal and vertical shifting alone cannot be achieved. While this behavior of the data is consistent at all temperatures, we choose here three curve segments from the 80°C data to illustrate this point in figure 11.

We have also attempted to extract a "glassy compliance" from these data to examine whether there is a rate or time dependent portion of this data that might obey a stress-shifting process[10]. This "glassy" compliance was represented by a monotonic function of the stress level (power law). While the curvature of the resulting creep segments changed over time, the net effect was such that both slope and curvature were measurably different for the creep segments so as to preclude horizontal (and vertical) shifting for constructing an unambiguous master curve[11].

[9]The increasing differences with higher temperatures may be due to the fact that the initial loading history has an effect. Although for linearly viscoelastic behavior data recorded after ten times the ramp time should be essentially free of transient response, this may not be true for the nonlinear behavior. All data presented here omit data recorded during the time from test start to ten times the ramp-up time (=one second).

[10]Schapery has pointed out that often the subtraction of a "glassy" compliance from the data leaves a "transient" (time dependent) portion that plots with constant slope on a log-log plot.

[11]We have also carefully re-examined Tervoort, Klompen and Govaert's (1996) data on uniaxial extension of Polycarbonate and arrived at similar results.

3.2 Axial creep response: We examine next the axial creep response in the presence of superposed torsion. This consideration is necessary for computing the influence on the maximum shear strain, discussed in the next section, and to illustrate that the axial strains are small compared to the shear strains. The contribution is on the order of $\epsilon_{xx}^2/(8\epsilon_{x\theta}^2)$ which, upon cursory data examination, amounts to about $1-2\%$. This observation is in accord with the observation that most of the nonlinear behavior of polymers is in the form of shear deformations, dilatational strains being typically very small. Like the shear strains, the axial strains were determined via digital image correlation. For reference purposes, we record in Figures 12-15 these normal strains at three temperatures (22, 50 and $100°C$), additional data being available in reference (Lu, 1997). Note that the uniaxial creep compliance is clearly sensitive to superposed shear deformations; also, considerably different creep rates result, depending on whether the axial load is tensile or compressive.

3.3 The effect of the first stress (strain) invariant on shear creep: It is thus clear that the axial stress exerts a marked influence on the shear creep. To demonstrate this, pure shear measurements at different temperatures were recorded as discussed above, and then the tests were repeated with a tensile or compressive axial stress added to the same shear load. The corresponding data[12] are displayed in figures 16-21, from where it is apparent that, at all temperatures considered, superposed (axial) tension and compression have a readily discernible and different effect on the creep behavior in shear. In each individual case represented in these figures the superposed axial loads possess equal magnitude, though a different sign. Thus the only difference between the combined response to a maximum (or octahedral) shear stress is the sign of the first stress invariant. To the extent that deformations are governed by small strain approximations, the same holds for the first strain invariant. A positive invariant produces always a higher creep rate than a negative one.

We observe further that at temperatures close to the glass transition the pure shear creep is intermediate to the data resulting from the positive and negative dilatation; this behavior does not hold at lower temperatures. One must observe, however, that for the records in figures 16-21 the pure shear response and the data incorporating additional normal stresses, the maximum (or octahedral) shear stresses are not the same. In fact, when normal stresses are added, the maximum shear stress for the stress states involving tension or compression is larger than for the pure shear case(s). One needs to investigate thus the response when the, say, maximum shear stress is the same, whether a dilatational component is absent or

[12]The data at each temperature are derived from a single specimen.

not.

This comparison is given in figures 22-25, so that in each of the four figures the compliances are determined for a constant maximum shear stress. In these figures the solid points represent direct creep measurements obtained on identical specimens. Curves identified by crosses have two sources: Those identified by a letter "b" are derived from specimens that were not part of the original material pool, while the curves identified by a letter "a" are derived from interpolating the isochronal data in figure 9. Where both tests and interpolation are available an average has been chosen for the response. While the data spread is not small, it is clear that the introduction of a common maximum shear stress brings the behavior above and below the glass transition to a common denominator in that the pure shear compliances generally fall between those that involve positive and negative first stress (strain) invariants. One observes thus that the magnitude of the deceleration or acceleration increases with temperature as ascertained from the increasing relative spread between the creep curves as one moves to higher temperatures.

It is clear that at all temperatures the pure shear data is intermediate to the curves for positive and negative stress invariants. Moreover, the acceleration or retardation due to positive or negative dilatation are of the same order. While the notion is thus close at hand that positive dilatation accelerates shear creep and negative dilatation retards it, the functional acceleration/retardation relation is yet do be determined. Certainly, free volume arguments are a possible start.

4 Summary

We have provided measurements of creep deformations under complex stress states comprising torsion with superposed axial tension or compression. There is a distinct effect of the dilatational component of the stress state on creep rates: Shear creep is sped up by positive dilatation and slowed by negative dilatation. As long as the maximum shear stress is the same, the acceleration and deceleration are about the same for identical absolute values of the dilatation component, giving response curves that are approximately symmetrical with respect to the pure shear responses. Definition of the onset of nonlinear viscoelastic behavior is possibly best defined in terms of isochronal plots, which determine that this behavior starts at about 0.5% shear strain for the PMMA studied here. Within experimental error, this value of a "critical shear strain" is invariant over the temperature range of $22 - 100°C$ studied here. This definition of onset of nonlinear behavior is synonymous with the onset of plastic deformation in metals (strain offset), and thus a possibly useful estimate for the

full linear/nonlinear material characterization of rigid polymers.

Acknowledgements: This work was initially supported by the program on Advanced Technologies (PAT) at Caltech under the sponsorship of Aerojet General, General Motors and TRW and by ONR grant N00014-91-J-1427 with Dr. Peter Schmidt as the monitor, later work was supported by NASA under grant #NSG 1483, with Dr. Tom Gates as the technical monitor. In addition, funds from the National Science Foundation under grant #CMS9504144 allowed completion of this study. Finally, the authors are indebted to Dr. Gregory B. McKenna for many relevant discussions in the past and during the preparation of this manuscript.

References

Bauwens-Crowet, C., 'The Compression Yield Behavior of Polymethyl Methacrylate Over a Wide Range of Temperatures and Strain-Rates', *Journal of Materials Science* **8**, 1973, 968

Bernstein, B., Kearsley, E.A. and Zapas, L.J., 'A Study of Stress Relaxation with Finite Strain',*Transactions of the Society of Rheology* **7**, 1963, 391

Brinson, L.C. and Gates, T.S., 'Effects of Physical Aging on Long Term Creep of Polymers and Polymer Matrix Composites',*International Journal of Solids and Structures* **32**, 1996, 827

Carapellucci, L.M. and Yee, A.F., 'The Biaxial Deformation and Yield Behavior of Bisphenol-A Polycarbonate: Effect of Anisotropy', Polymer Engineering and Science **26**, 1986, 920

Duran, R.S. and McKenna, G.B., 'A Torsional Dilatometer for Volume Change Measurements on Deformed Glasses: Instrument Description and Measurements on Equilibrated Glasses',*Journal of Rheology* **34**, 1990, 813

Ewing, P.D., Turner, S. and Williams, J.G., 'Combined Tension-Torsion Studies on Polymers: Apparatus and Preliminary Results for Polythene', *Journal of Strain Analysis*, **7**, 1972, 9

Ewing, P.D., Turner, S. and Williams, J.G., 'Combined Tension-Torsion Creep of Polythene with Abrupt Changes of Stress', *Journal of Strain Analysis* **8**, 1973, 83

Fillers, R.W. and Tschoegl, N.W., 'The Effect of Pressure on the Mechanical Properties of Polymers', *Transactions of the Society of Society of Rheology* **21**, 1977, 51

Hasan, O.A. and Boyce, M.C., 'A Constitutive Model for the Nonlinear Viscoelastic Viscoplastic Behavior of Glassy Polymers,' *Polymer Engineering and Science* **35**, 1995, 3314

Knauss, W.G., 'On the Steady Propagation of a Crack in a Viscoelastic Sheet: Experiments and Analysis,' *Deformation & Fracture of High Polymers*, Kausch, Hassell and Jaffe (Eds.), Penum Press, 1974,

Knauss, W.G. and Emri, I., 'Non-linear Viscoelasticity Based on Free Volume Consideration,' *Computer & Structures* **13**, 1981, 123

Knauss, W.G. and Emri, I., Volume Change and the Nonlinearly Thermo-Viscoelastic Constitution of Polymers, *Polymer Engineering and Science* **27**, 1987, 86

Knauss, W.G. and Kenner V.H., 'On the Hygrothermomechanical Characterization of Polyvinyl Acetate', *Journal of Applied Physics* **51**, 1980, 5131

Lee, A. and McKenna, G.B., 'The Physical Ageing Response of an Epoxy Glass Subjected to Large Stresses', *Polymer* **31**, 1990, 423

Lide, D.R., *CRC Handbook of Chemistry and Physics*, CRC Press, 1995, 15

Lou, Y.C. and Schapery, R.A., 'Viscoelastic Characterization of a Nonlinear Fiber-Reinforced Plastic', *Journal of Composites Materials* **5**, 1971, 208

Losi, G.U. and Knauss, W.G., 'Free Volume Theory and Nonlinear Thermoviscoelasticity', *Polymer Science and Engineering*, **32**, 1992, 542

Lu, H., 'Nonlinear Thermo-Mechanical Behavior of Polymers under Multiaxial Loading', *Ph.D. thesis*, California Institute of Technology, Pasadena, California, USA, 1997

Lu, H., Zhang, X. and Knauss, W.G., 'Uniaxial, Shear, and Poisson Relaxation and Their Conversion to Bulk Relaxation: Studies on Poly(Methyl Methacrylate)', *Polymer Engineering and Science* **37**, 1997, 1053

Lu, H., Vendroux, G. and Knauss, W.G., 'Surface Deformation Measurements of a Cylindrical Specimen by Digital Image Correlation', *Experimental Mechanics* **37**, 1997, 433

Lustig, S.R., Shay, R.M. and Caruthers, J.M., 'Thermodynamic Constitutive Equations for Materials with Memory on a Material Time-Scale', *Journal of Rheology* **40**, 1996, 69

McKenna, G.B., 'On the Physics Required for Prediction of Long Term Performance of Polymers and their Composites', Journal of Research of NIST **99**, 1994, 169

McKenna, G.B., personal communications, 1999

McKenna, G.B. and Zapas, L.J., 'Nonlinear Viscoelastic Behavior of Poly(methyl methacry-

late) in torsion', *Journal of Rheology* **23**, 1979, 151

Moonan, W.K. and Tschoegl, N.W., 'Effect of Pressure on the Mechanical Properties of Polymers. 2. Expansivity and Compressibility Measurements', *Macromolecules* **16**, 1983, 55

Moonan, W.K. and Tschoegl, N.W., 'Effect of Pressure on the Mechanical Properties of Polymers. 3. Substitution of the Glassy Parameters for Those of the Occupied Volume', *International Journal of Polymer Materials* **10**, 1984, 199

Moonan, W.K. and Tschoegl, N.W., 'Effect of Pressure on the Mechanical Properties of Polymers. 4. Measurements in Torsion', *Journal of Polymer Science, Part B, Polymer Physics*, **23**, 1985, 623

Müller, H.K. and Knauss, W.G., 'Crack Propagation in a Linearly Viscoelastic Strip', *Journal of Applied Mechanics* **38**, Series E, 1971, 483

Murnahan, F.D., *Finite Deformation of Elastic Solid*, Wiley, New York, 1951, 130

O'Connell, P.A. and McKenna, G.B., 'Large Deformation Response of Polycarbonate: Time-Temperature, Time-Aging Time, and Time-Strain Superposition', *Polymer Engineering and Science*, **37**, 1997, 1485

Povolo, F. and Hermida, E.B., 'Phenomenological Description of Strain Rate and Temperature-Dependent Yield Stress of PMMA', *Journal of Applied Polymer Science* **58**, 1995, 55

Santore, M.M., Duran, R.S. and McKenna, G.B., 'Volume Recovery in Epoxy Glasses Subjected to Torsional Deformation–the Question of Rejuvenation', *Polymer* **32**, 1991, 2377

Schapery, R.A., 'Further Development of a Thermodynamic Constitutive Theory: Stress Formulation', Purdue University, 1969, Report 69-2

Schapery, R.A., 'A Theory of Crack Initiation and Growth in Viscoelastic Media: I. Theoretical Development', II. Approximate Methods of Analysis' and III. Analysis of Continuous Growth', *International Journal of Fracture* **11**, 141-159.; **11**, 369-388; **11**, 1975, 549

Sternstein, S.S. and Ongchin, L., 'Yield Criteria for Plastic Deformation of Glassy High Polymers in General Stress Fields', *American Chemical Society: Polymer Preprints* **10**, 1969, 1117

Struik, L.C.E., *Physical Aging in Amorphous Polymers and Other Materials*, Elsevier Scientific Publishing Company, 1978

Sutton, M.A., Wolters, W.J., Peters, W.H., Rason, W.F. and McNeil, S.R., 'Determination of Displacement Using an Improved Digital Correlation Method', *Image Vision Computing*

1, 1983, 133

Tervoort, T.A., Klompen, E.T.J. and Govaert, L.E., 'A multi-mode approach to finite, three-dimensional nonlinear viscoelastic behavior of polymer glasses', *Journal of Rheology* 40, 1996, 779

Thorkildsen, R.L., *Engineering Design for Plastics*, E. Baer, ed., Reinhold, NY, 1964

Wineman, A., S. and Waldron, W.K., Jr., 'Yieldlike Response of a Compressible Nonlinear Viscoelastic Solid,' *Journal of Rheology* **39**, 1995, 401

Williams, M.L., Landel, R.F., Ferry, J.D., 'The Temperature Dependence of Relaxation Mechanisms in Amorphous Polymers and Other Glass-forming Liquids', *Journal of the American Chemical Society* **77**, 1955, 3701

Zapas, L.J., McKenna, G.B. and Brenna, A., 'An analysis of the Corrections to the Normal Force Response for the Cone and Plate Geometry in Single-Step Stress Relaxation Experiments', Journal of Rheology **33**, 1989, 69

List of Figures

Figure 24: Shear Creep Compliance at $80°C$ Evaluated in Terms of the Maximum Engineering Shear Strain and Maximum Shear Stress

Figure 25: Shear Creep Compliance at $100°C$ Evaluated in Terms of the Maximum Engineering Shear Strain and Maximum Shear Stress

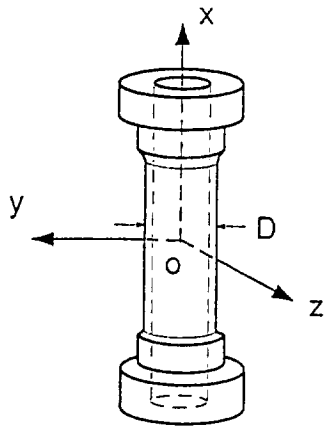

Figure 1: Thin-Walled Cylindrical Specimen

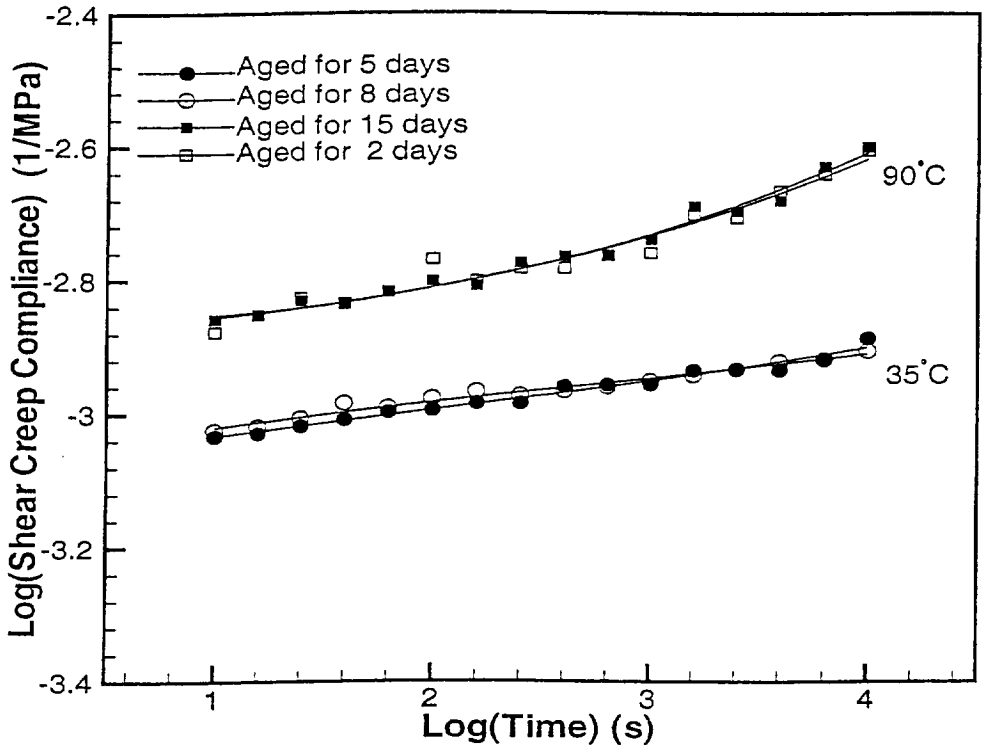

Figure 2: Shear Creep Compliances at 35°C and 90°C: Results of Ageing Studies

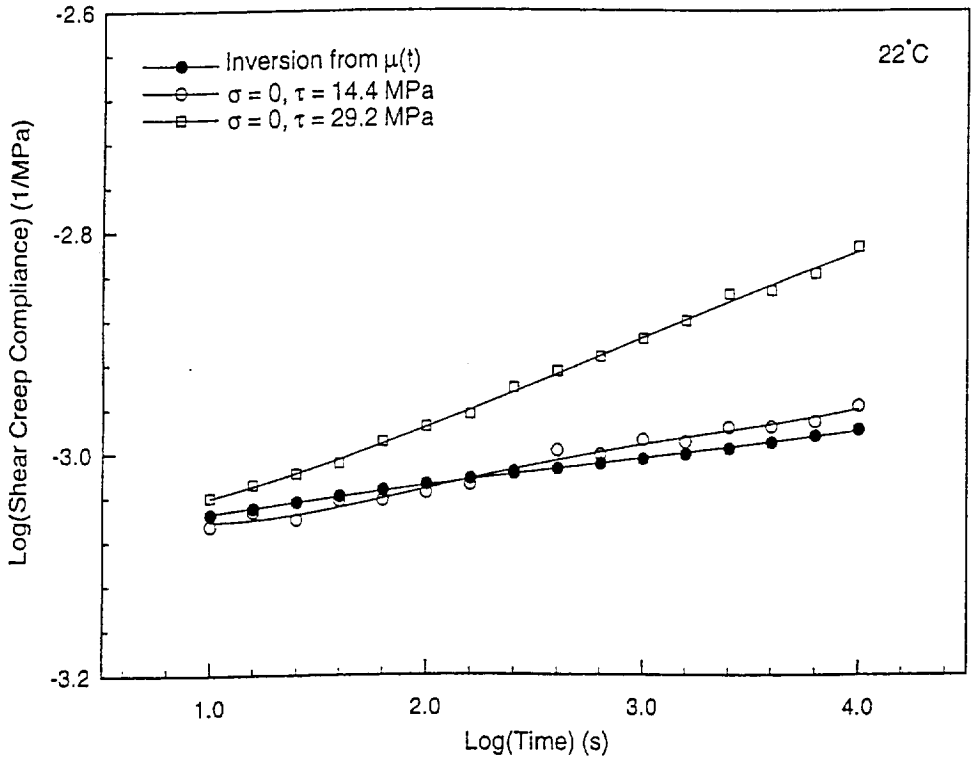

Figure 3: Shear Creep Compliance at 22°C

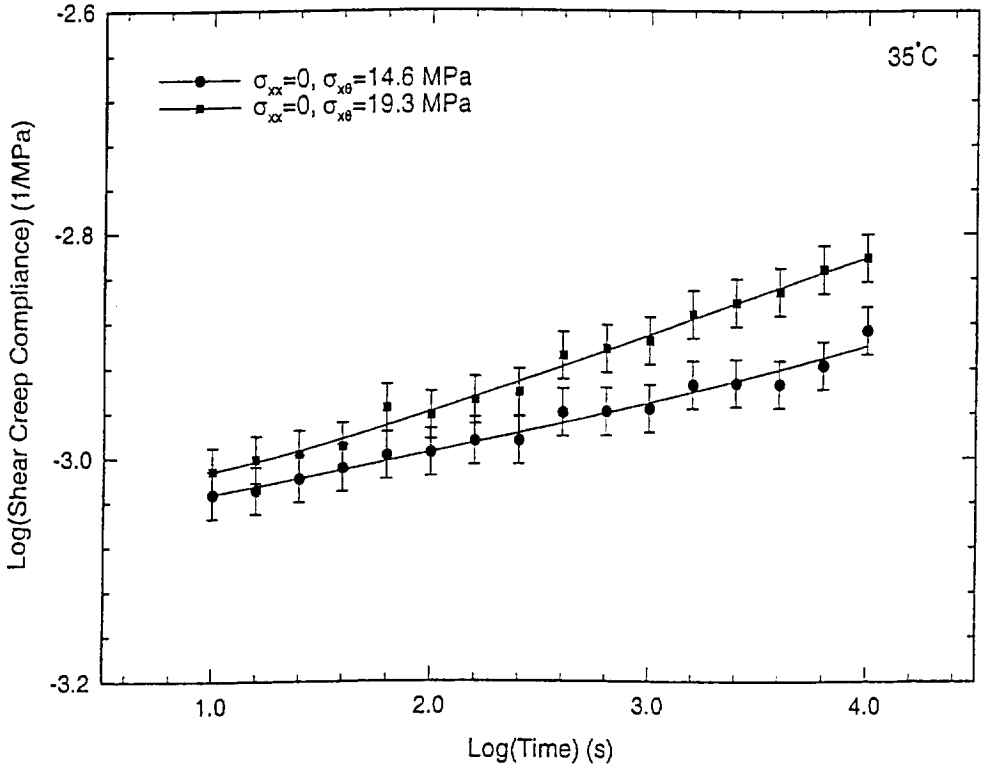

Figure 4: Shear Creep Compliance at 35°C

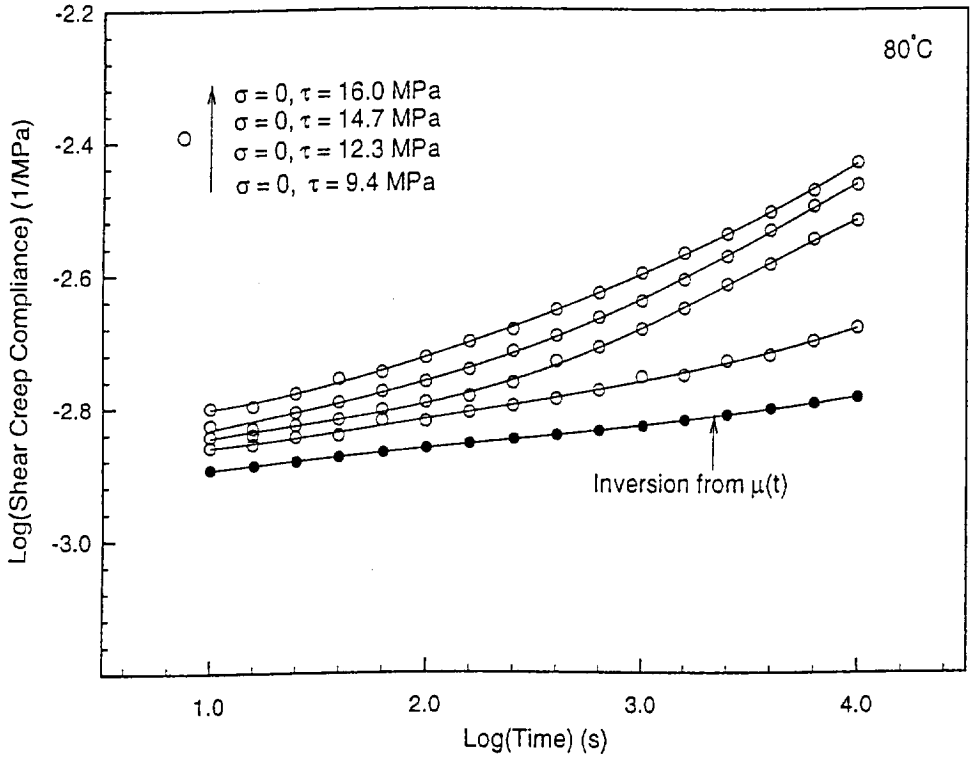

Figure 5: Shear Creep Compliance at 80°C

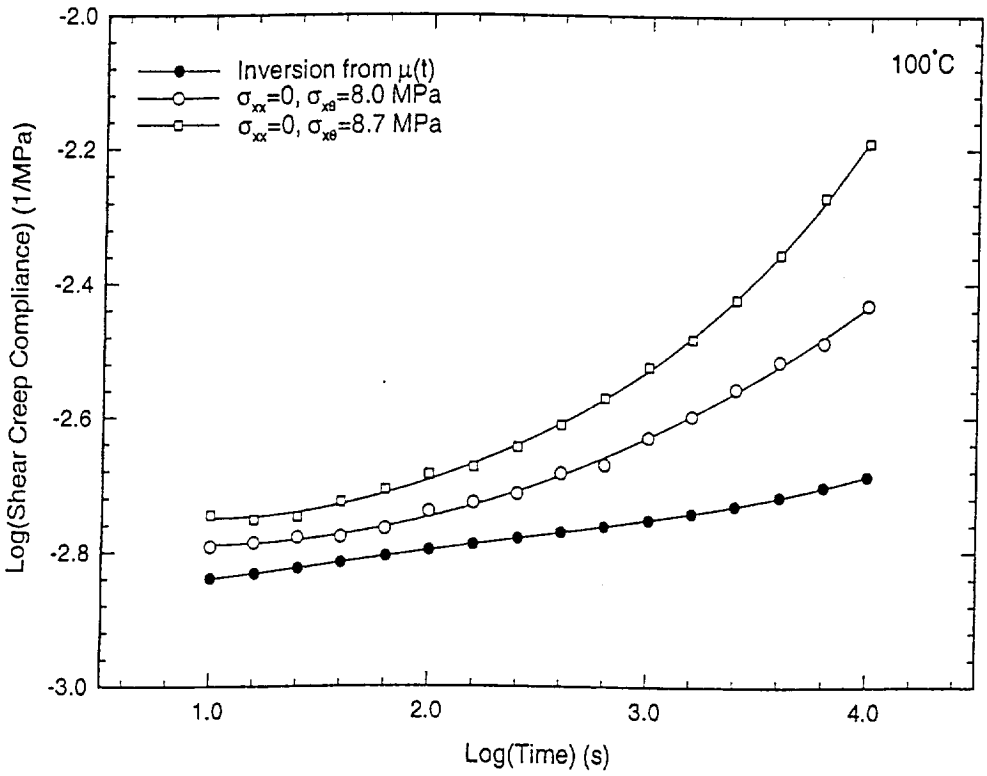

Figure 6: Shear Creep Compliance at $100°C$

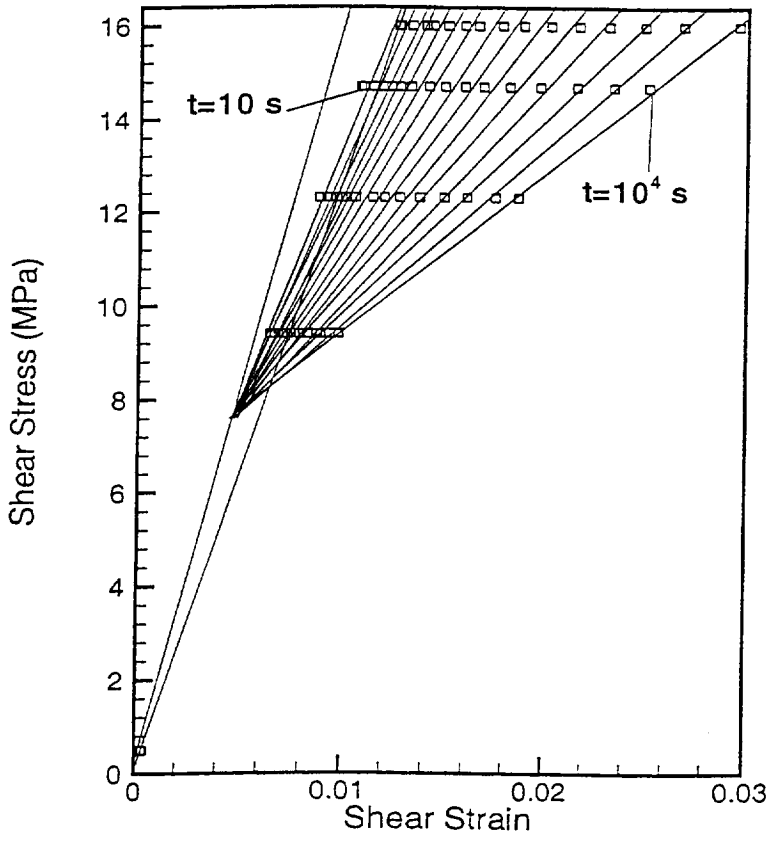

Figure 7: Isochronic Shear Stress-Shear Strain Relation at $80°C$

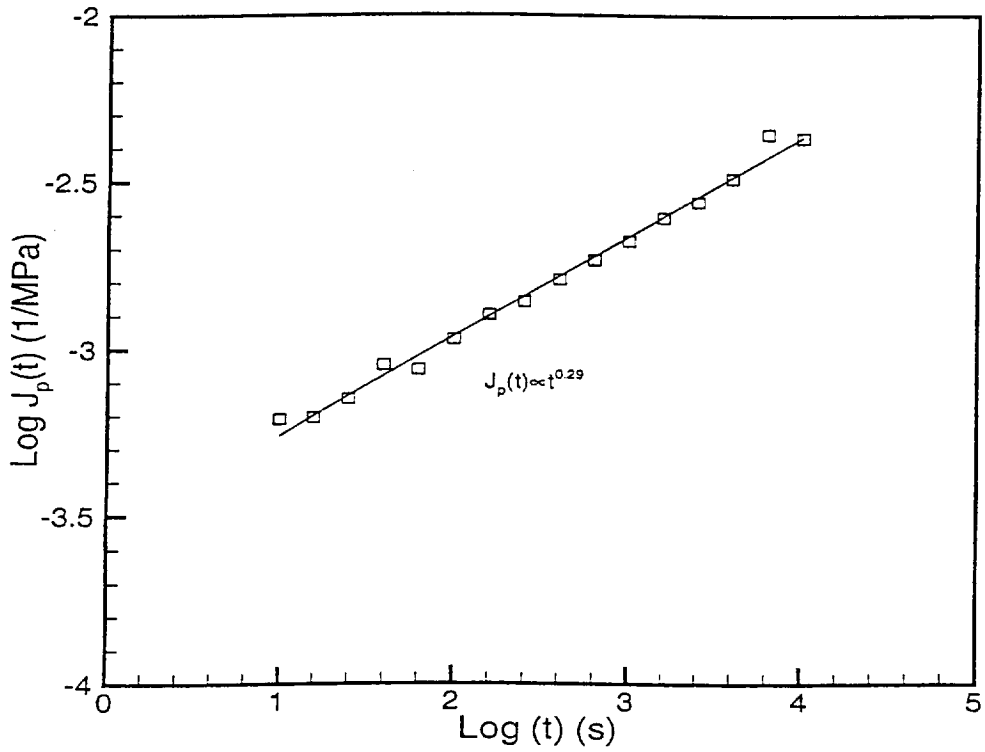

Figure 8: $J_p(t)$ at $80°C$

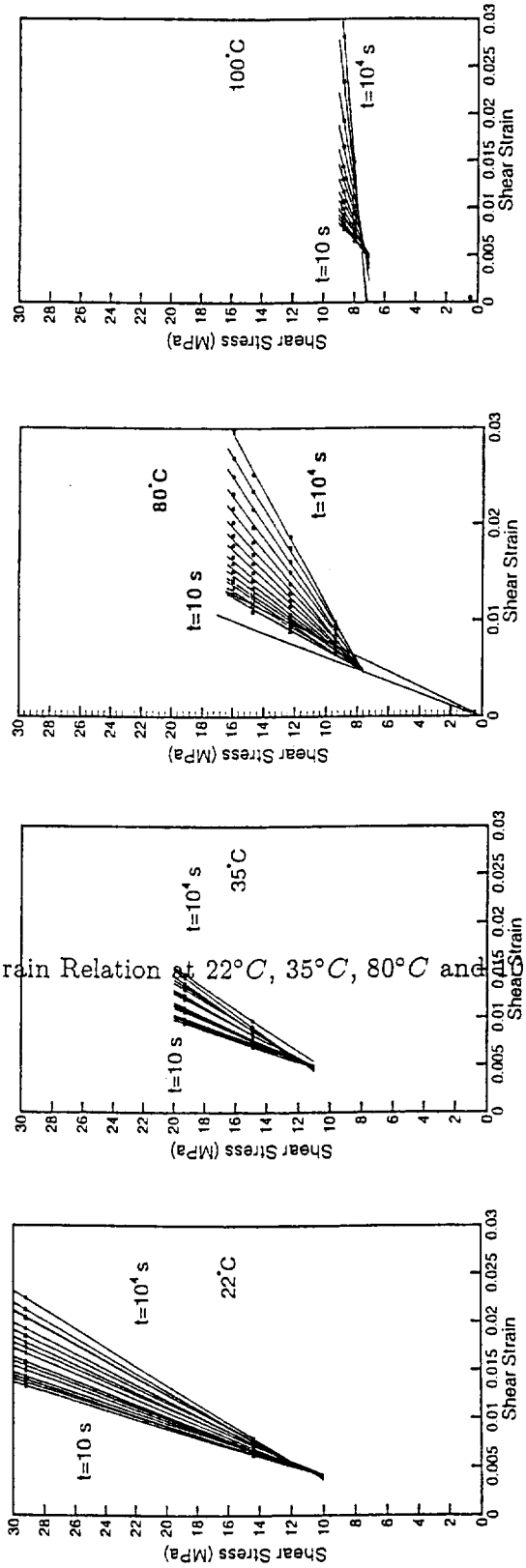

Figure 9: Isochronic Shear Stress-Shear Strain Relation at $22°C$, $35°C$, $80°C$ and $100°C$

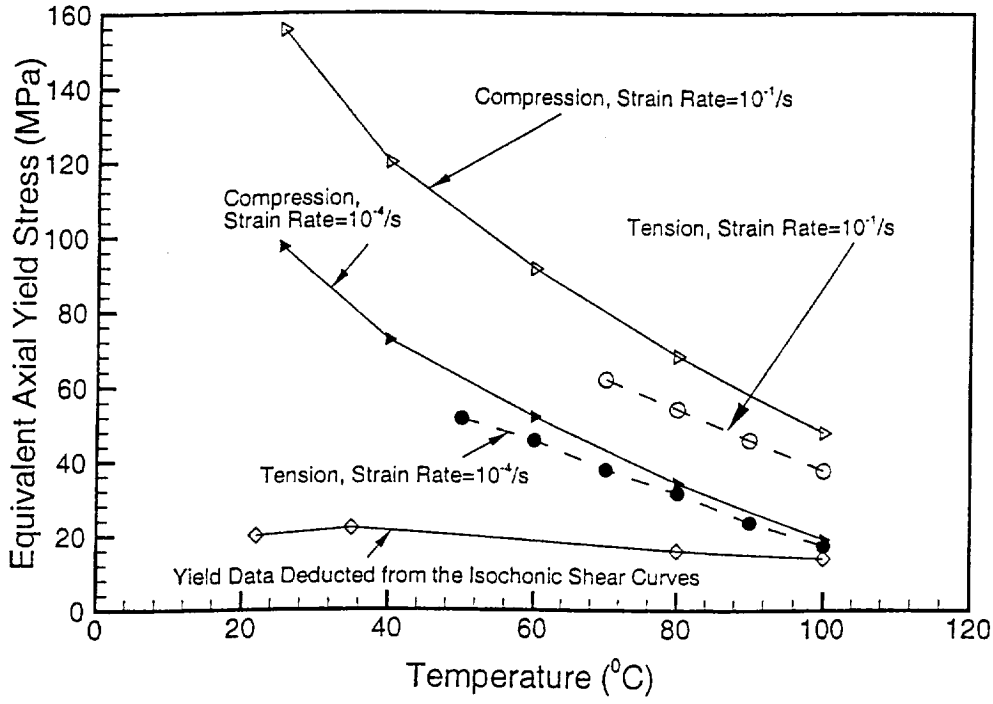

Figure 10: Yield Behavior (Equivalent Multiaxial Stress State) of PMMA at Different Temperatures and Deformation Histories: Deduced from Creep and Uniaxial Compression or Tension at $10^{-1}/sec$ and $10^{-4}/sec$

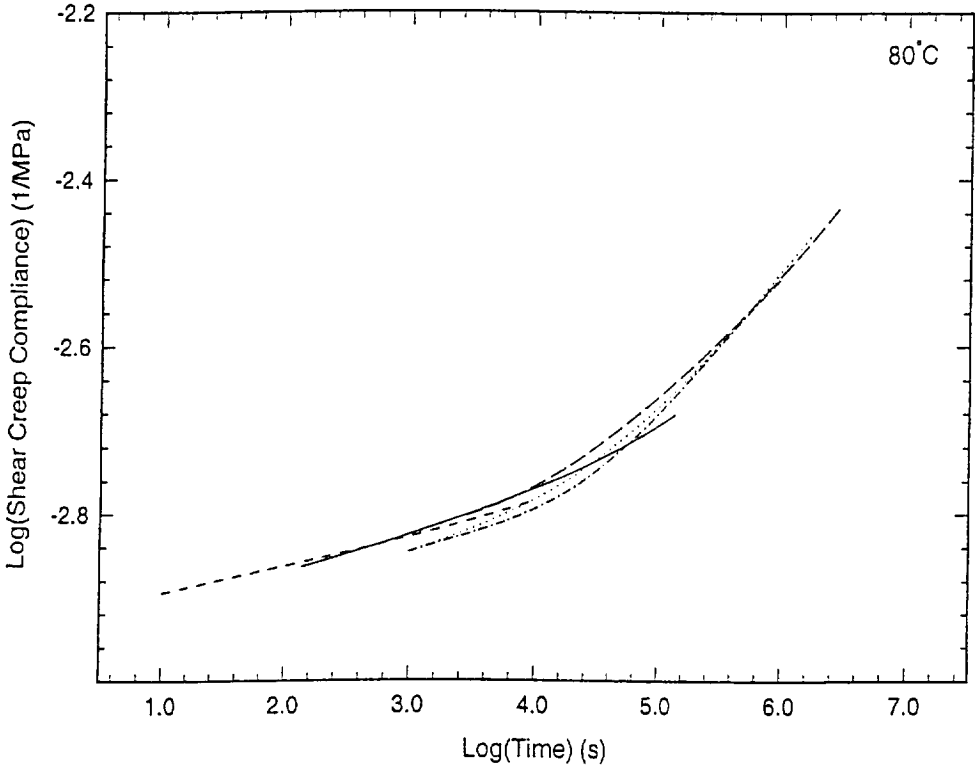

Figure 11: Horizontal Shifting of Shear Creep Compliances at 80°C

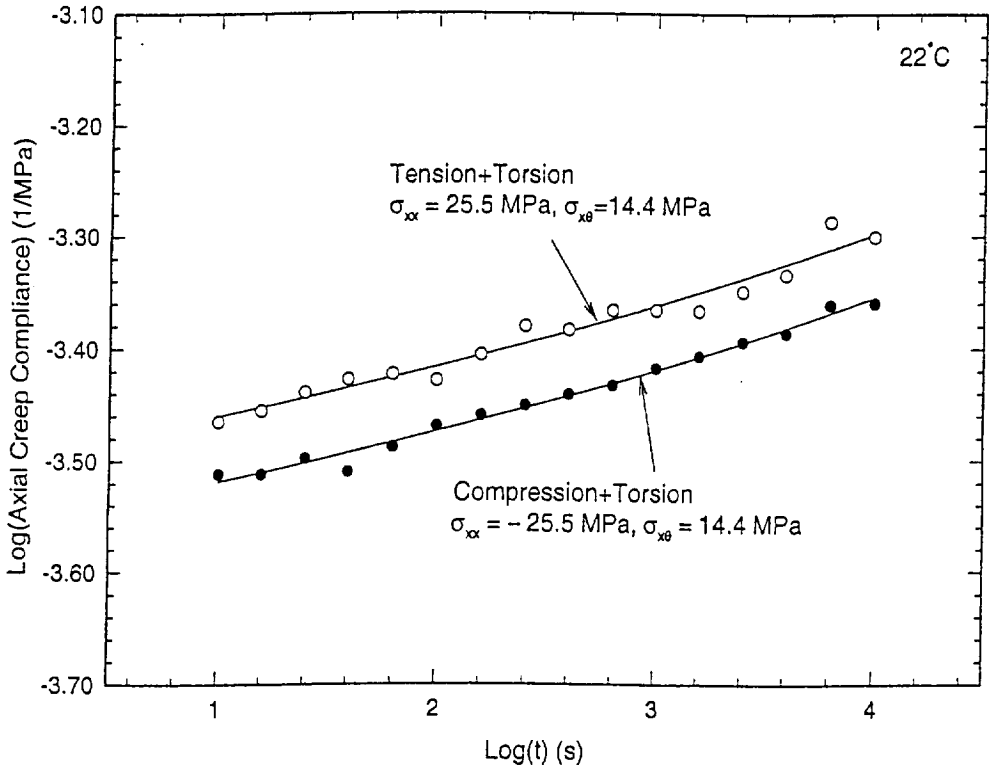

Figure 12: Axial Creep Compliance at 22°C

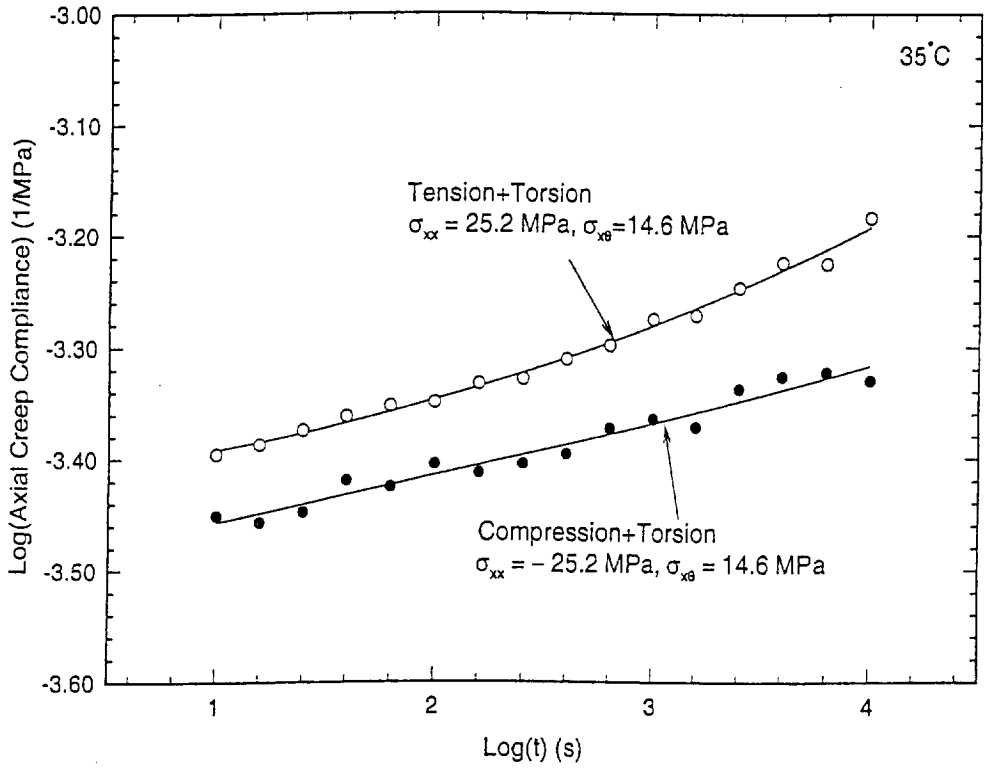

Figure 13: Axial Creep Compliance at 35°C

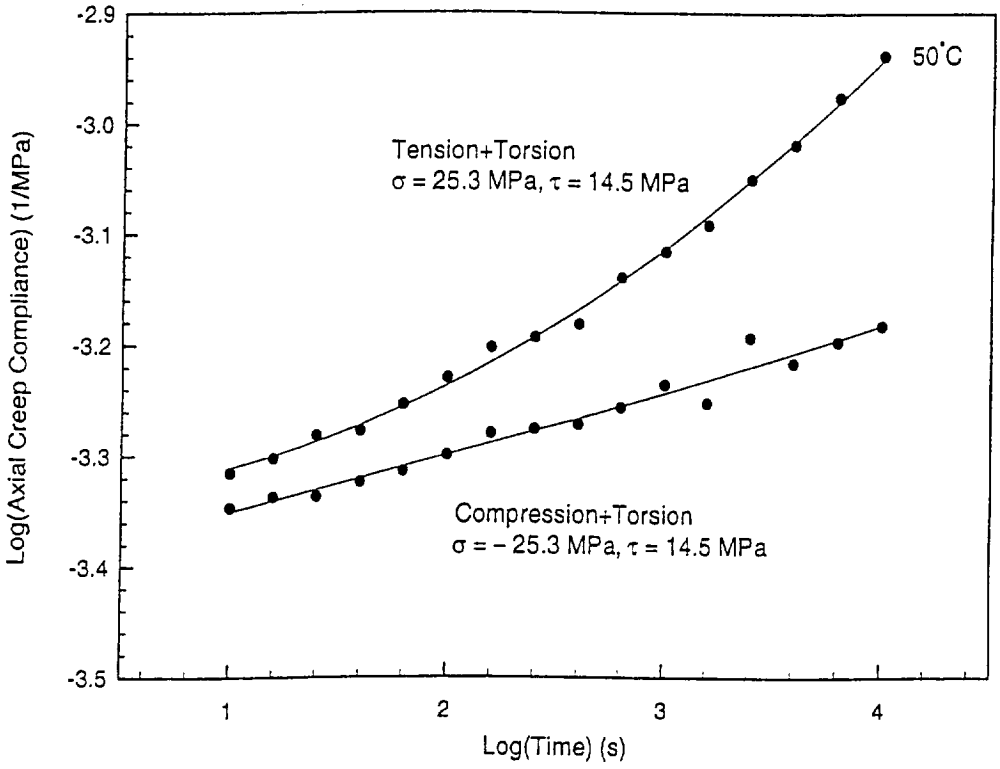

Figure 14: Axial Creep Compliance at 50°C

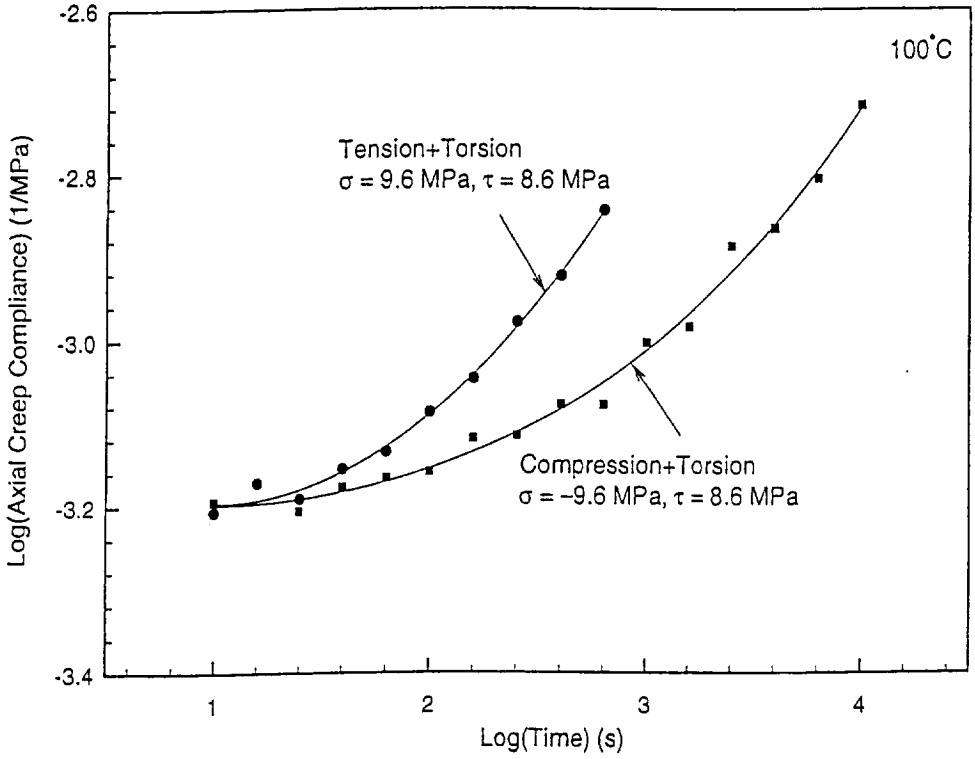

Figure 15: Axial Creep Compliance at 100°C

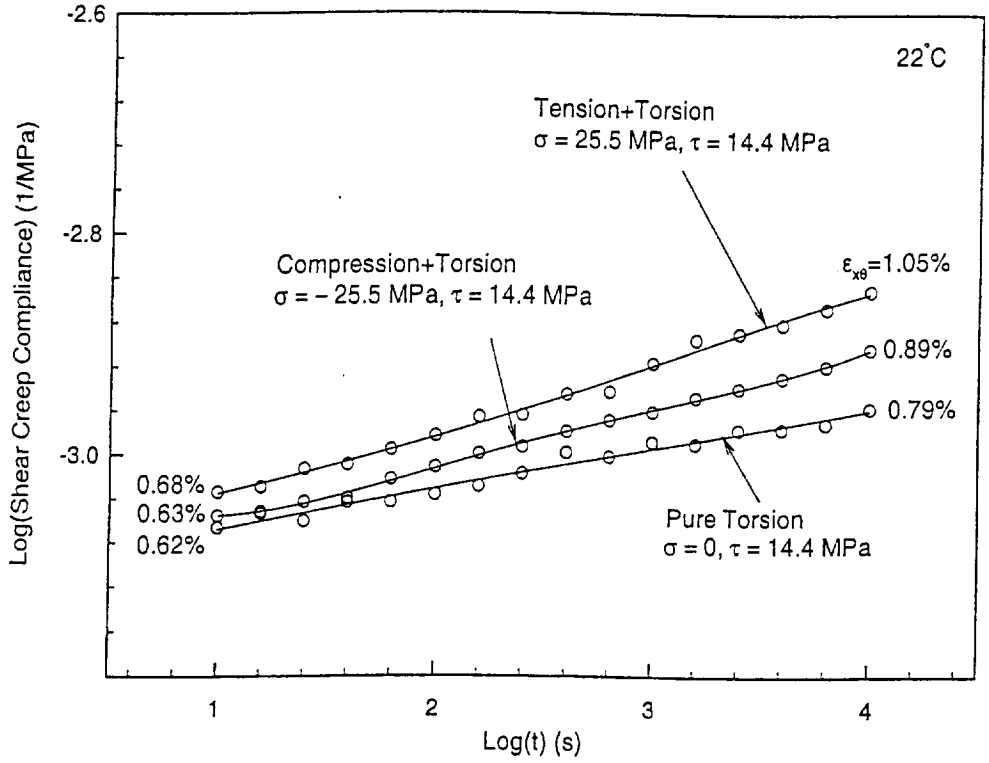

Figure 16: Shear Creep Compliance at $22°C$

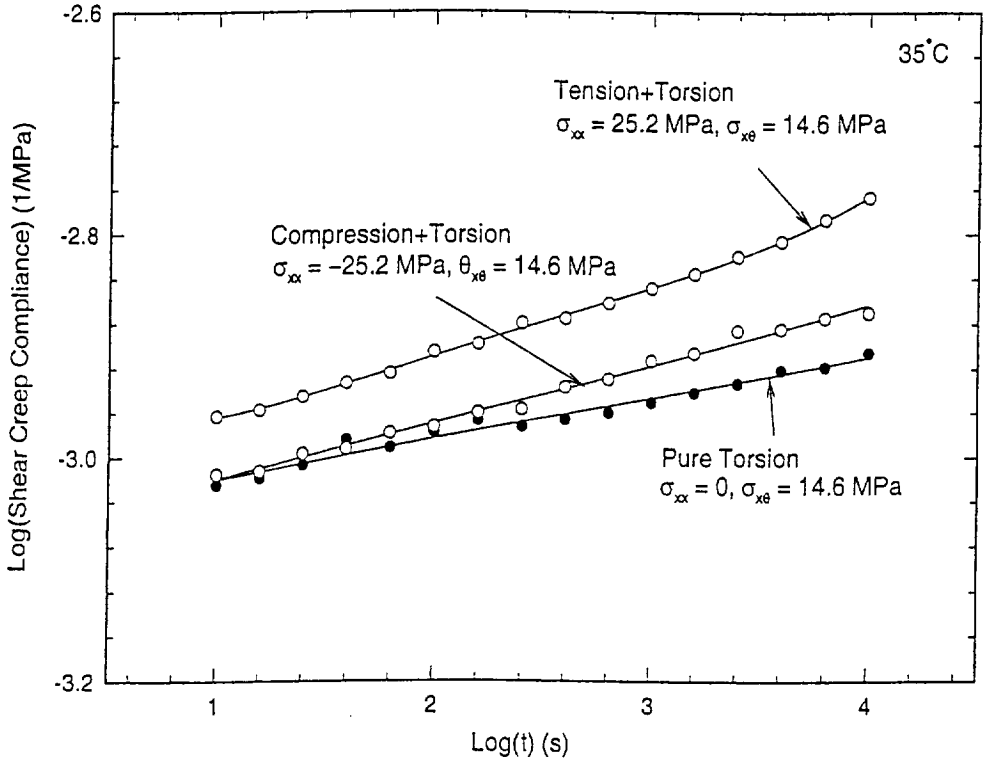

Figure 17: Shear Creep Compliance at 35°C

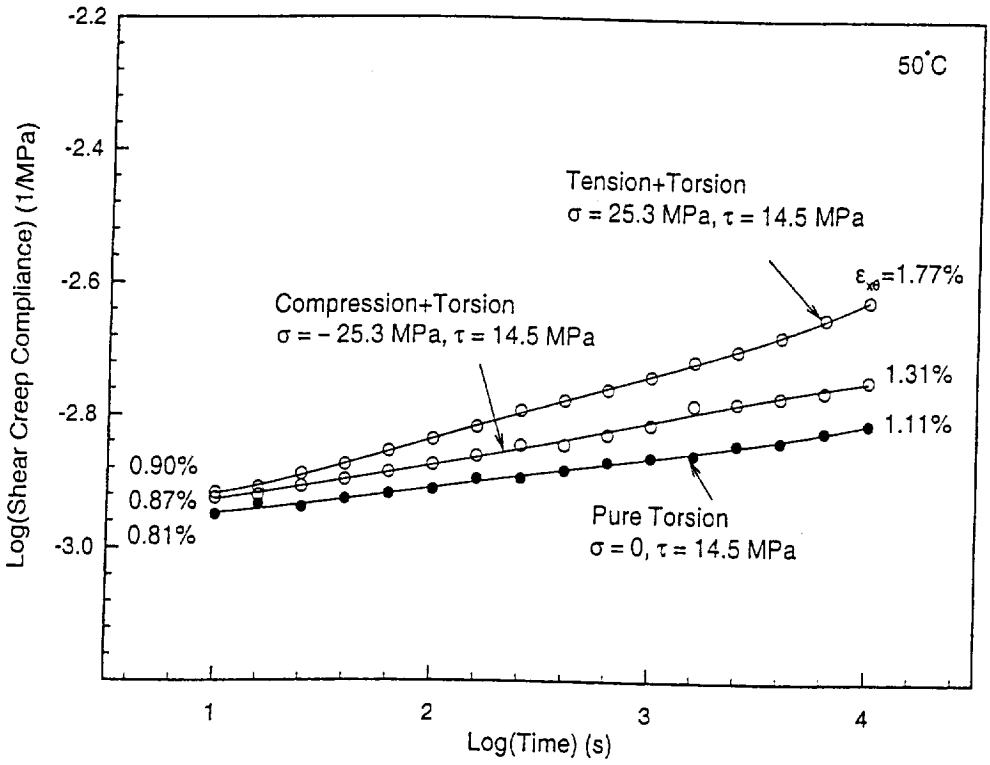

Figure 18: Shear Creep Compliance at $50°C$

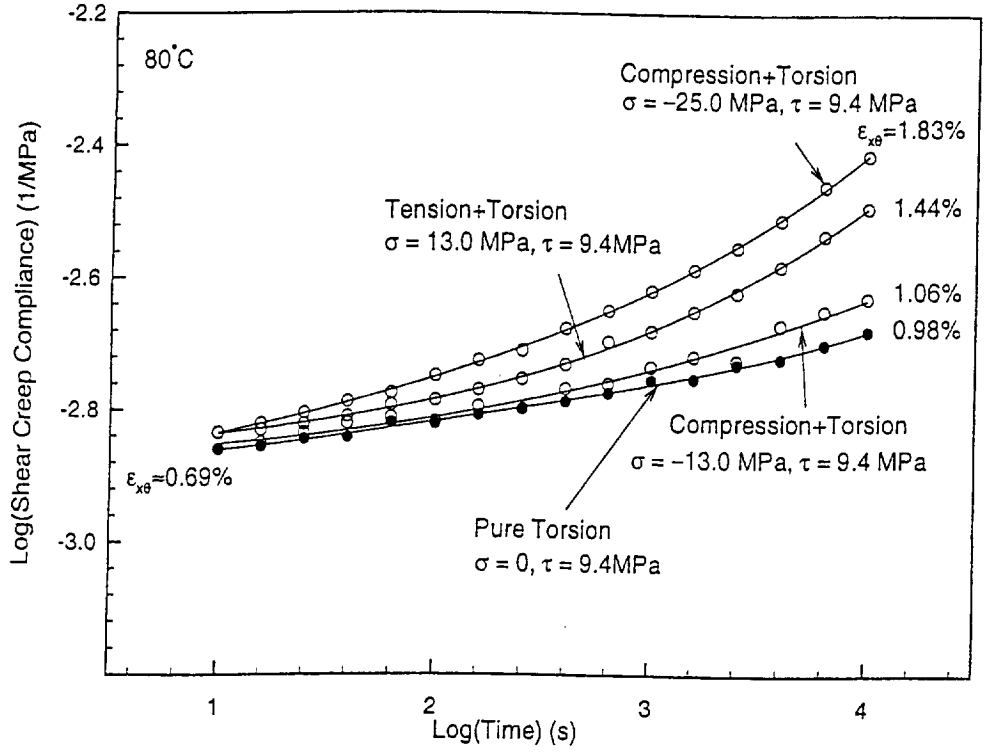

Figure 19: Shear Creep Compliance at 80°C

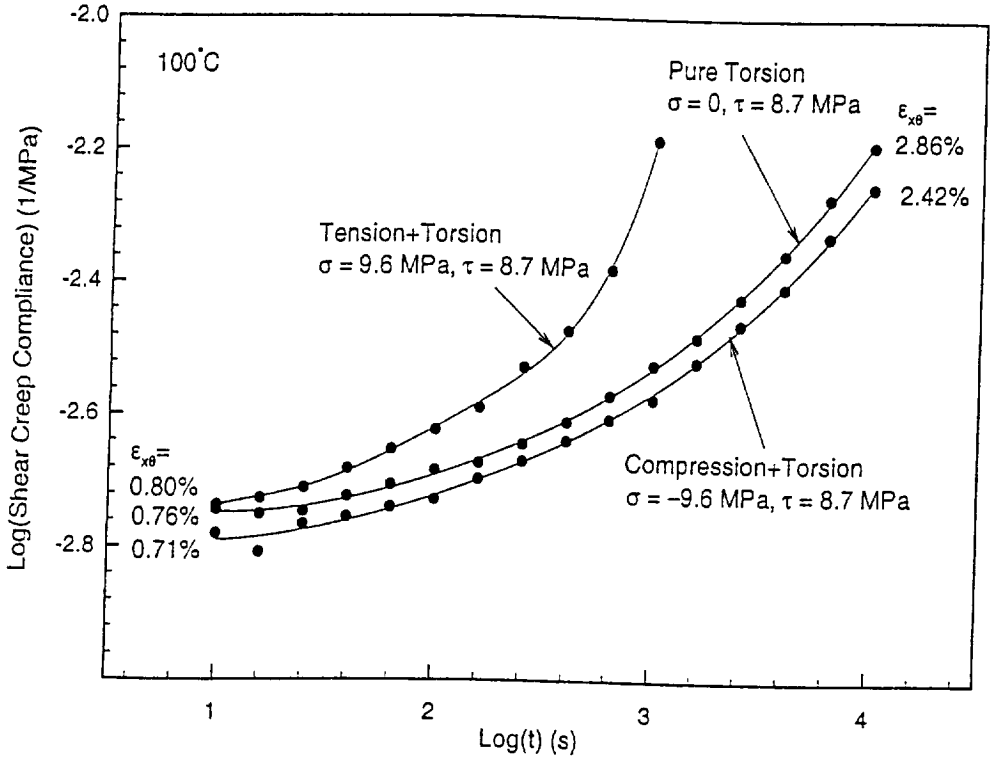

Figure 20: Shear Creep Compliance at 100°C

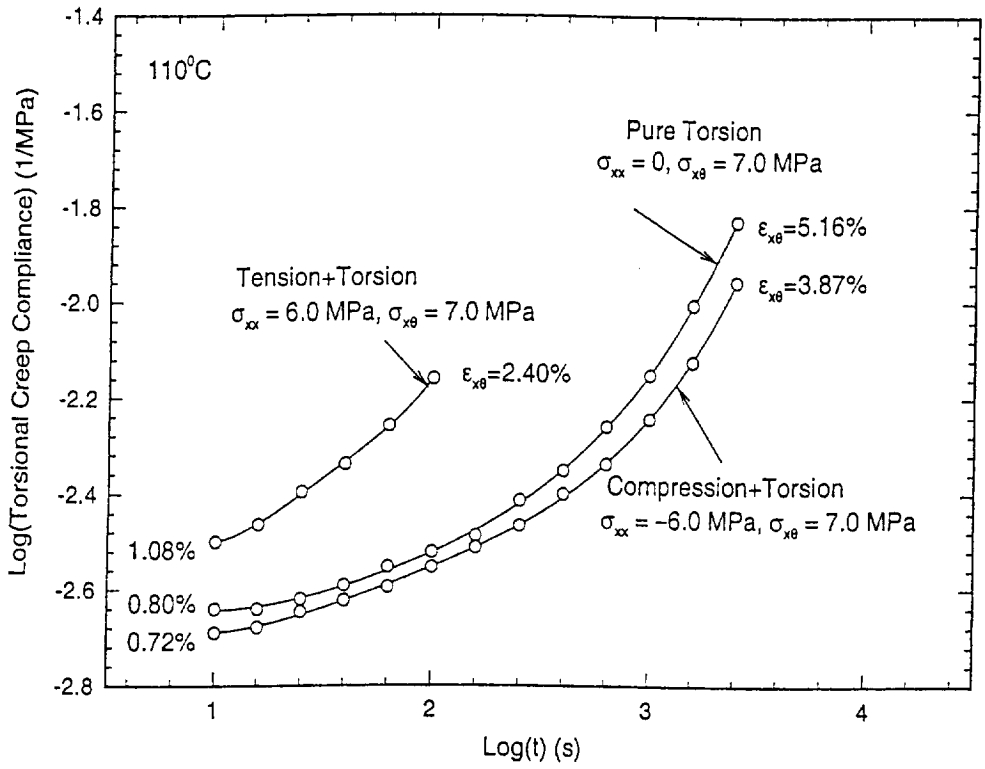

Figure 21: Shear Creep Compliance at $110°C$

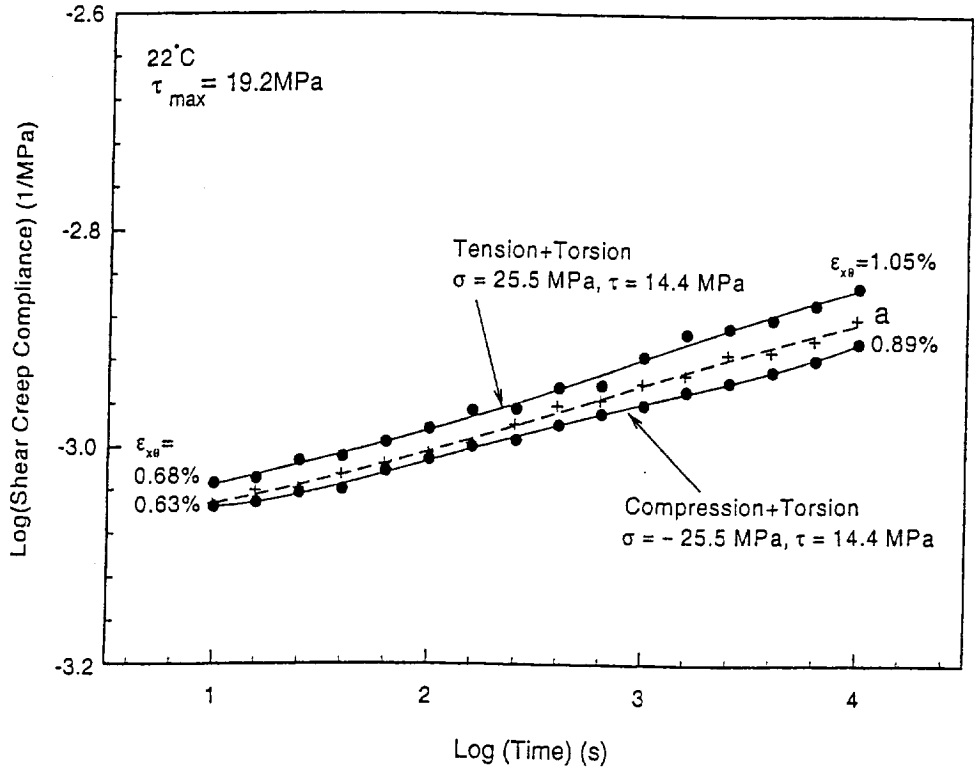

Figure 22: Shear Creep Compliance at 22°C Evaluated in Terms of the Maximum Engineering Shear Strain and Maximum Shear Stress

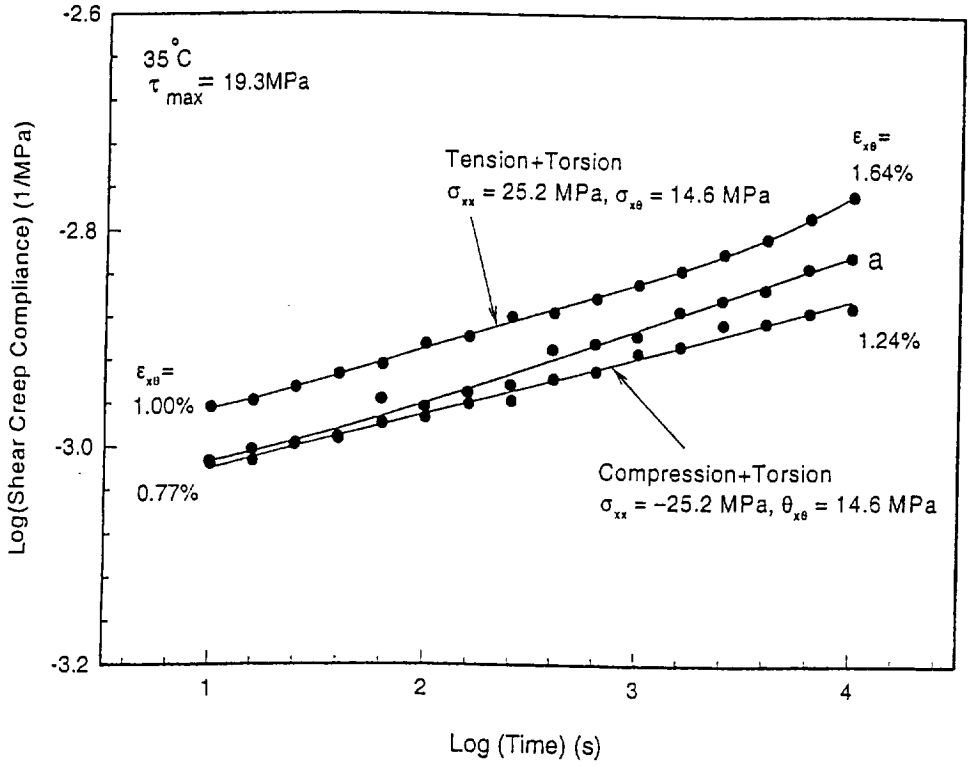

Figure 23: Shear Creep Compliance at 35°C Evaluated in Terms of the Maximum Engineering Shear Strain and Maximum Shear Stress

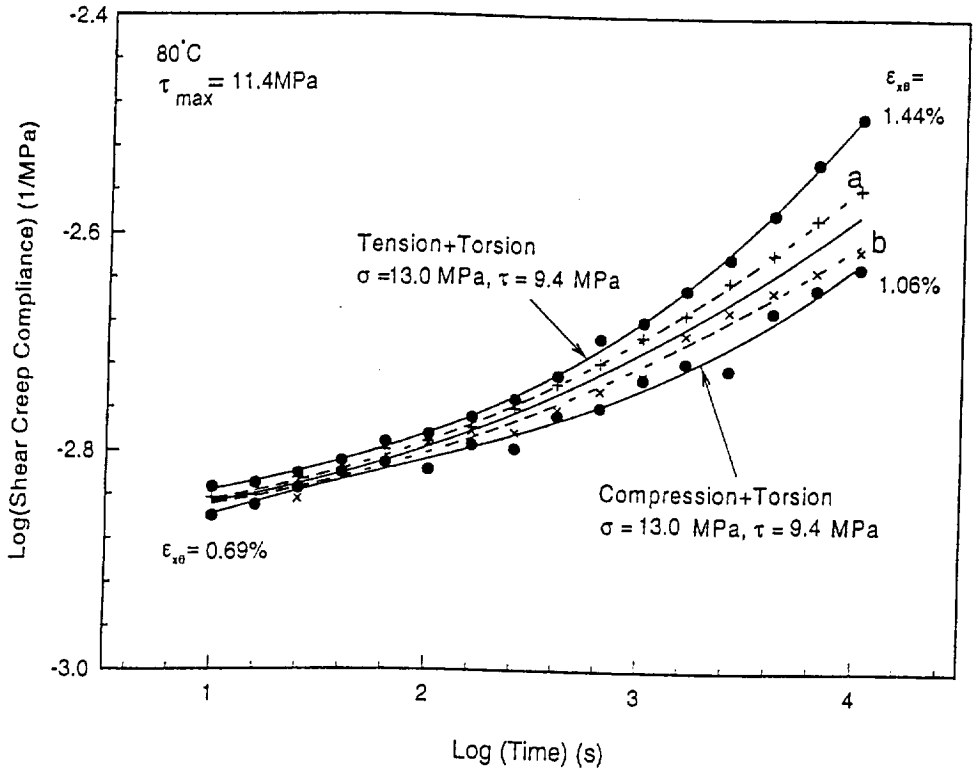

Figure 24: Shear Creep Compliance at 80°C Evaluated in Terms of the Maximum Engineering Shear Strain and Maximum Shear Stress

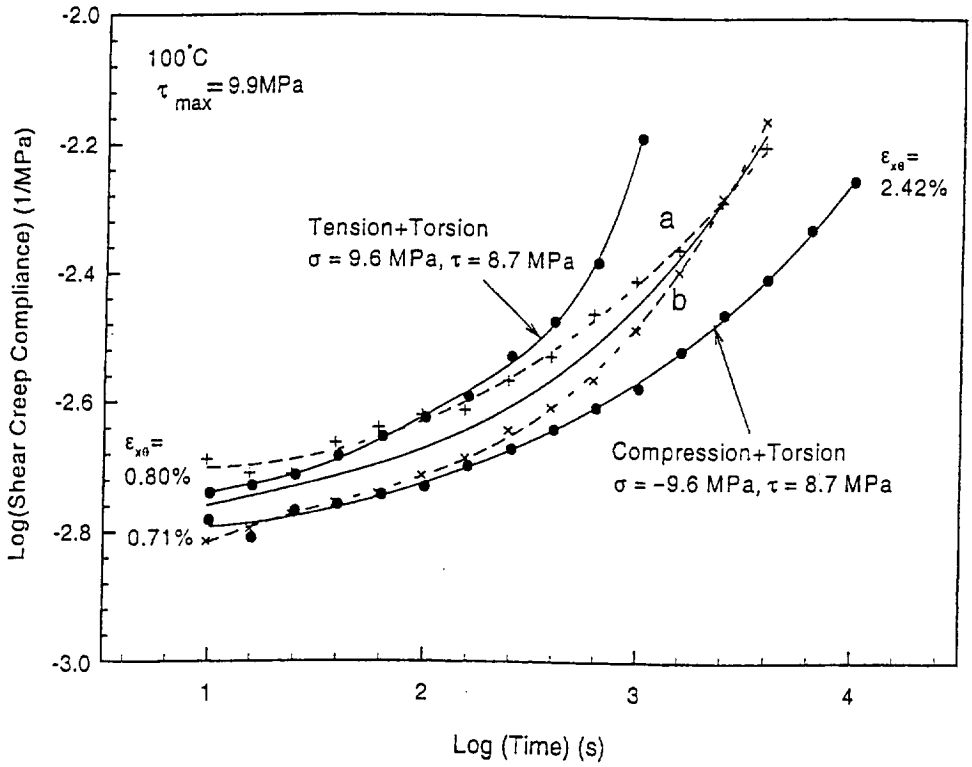

Figure 25: Shear Creep Compliance at 100°C Evaluated in Terms of the Maximum Engineering Shear Strain and Maximum Shear Stress

Mechanics of Time-Dependent Materials 1: 33–49, 1997.

The Temperature and Frequency Dependence of the Bulk Compliance of Poly(Vinyl Acetate). A Re-Examination

T.H. DENG and W.G. KNAUSS
Graduate Aeronautical Laboratories, California Institute of Technology, Pasadena, CA 91125, U.S.A.

(Received 22 November 1996; accepted 27 November 1996)

Abstract. Measurements are described and analyzed for the determination of the dynamic bulk compliance for Poly(vinyl acetate) [PVAc] as a function of frequency and temperature at atmospheric pressure to generate a master compliance curve over a total frequency range of about 12 decades. Measurements are based on the compressibility of a specimen confined to an oil-filled cavity resulting from pressurization by a piezoelectric driver and response of a like receiver. Experimental problems addressing limitations in resolution capability are discussed. The results are compared with the classical measurements obtained by McKinney and Belcher over thirty years ago. Further comparison of the bulk with shear compliance data shows that the extent of the transition ranges for the two material functions are comparable, but the two transitions belong to different time scales, that of the bulk response falling mostly into the glassy domain of the shear behavior. One concludes thus that for linearly viscoelastic response the molecular mechanisms contributing to shear and bulk deformations have different conformational sources.

Key words: dynamic bulk compliance, dynamic bulk modulus, linearly viscoelastic properties, Poly(vinyl acetate)

1. Introduction

The theory of linear viscoelasticity has been formulated and used for several decades along with the identification of the requisite material functions. There are many polymer systems for which relaxation or creep data for either uniaxial or shear response have been measured, and their number is too large to warrant even a partial listing here. By contrast, during this time span the determination of the time dependent bulk (volumetric) response has been surprisingly limited to essentially a single investigation (McKinney and Belcher, 1963) which covers a similarly large time or frequency range. This exceedingly sparse set of investigations into the bulk behavior of polymers is not so much the consequence of relative unimportance, as it is of the extreme difficulties associated with making sufficiently precise measurements of very small deformations. It is, therefore, with much respect that we refer to the work of McKinney and Belcher who have made such measurements in their time with instrumentation that, while sparingly described in their publication, belongs to a time of lesser sophistication than is typical of our electronics-governed

age. One particular question surrounding the work of McKinney and Belcher is the unusually low glass transition temperature reported for their material: While that temperature is usually recorded as being around 30°C, McKinney and Belcher determined this value as 16.9°C. Their material may have been a specially compounded PVAc.

The result of the McKinney and Belcher investigation showed that the magnitude of the bulk response changes by a relatively small factor through the transition range as compared to a factor of one hundred to a thousand for the uniaxial or shear behavior, excluding the long-term flow region for uncrosslinked polymers. If one trusts the time-temperature superposition principle (we use it in the sequel), these findings have been confirmed qualitatively by Lin and Nolle (1989) who measured the bulk response by a nearly identical method, but essentially only as a function of the temperature, inasmuch as the frequency range was very small. Similar measurements over six decades of frequencies at room temperature on 42 different polymers by Heydemann (1959) established typically very small variations or constancy of bulk response for these limited conditions.

In applications of the linear theory of viscoelasticity to engineering problems the limited knowledge of time dependent bulk response has not been a severe impediment inasmuch as the assumptions of a constant bulk modulus or compliance has served (engineering) analysts well. However, more recent studies addressing nonlinearly viscoelastic behavior have pointed to the potential need for a more careful characterization of bulk response. Specifically, it has been demonstrated that the dilatational behavior of polymers can have a significant effect on the time dependent shear or uniaxial response once the small deformation range (strains less than about 0.2%) is exceeded. It appears that outside of this small strain range the mutual independence of bulk and shear response ceases, and initial (free volume) models pointed to the need to better understand the bulk response throughout the transition range (Knauss and Emri, 1981, 1987; Losi and Knauss, 1992). Also studies on nonlinearly viscoelastic behavior involving the interdependency of dilatational and shear deformations on time dependent response reinforced that observation (Duran and McKenna, 1990), though in other studies the nonlinearly viscoelastic behavior has been found to involve an intrinsically nonlinear shear component in addition to the coupling between the volumetric and shear effects (Lu and Knauss, 1997).

In this paper we delineate the measurement of rate dependent bulk response by describing first the experimental apparatus, along with issues requiring special attention in the pursuit of similar studies in Section 2 and its calibrations in Section 3. The results of the measurements are recorded and compared with those of McKinney and Belcher, as well as with the transition range for the shear response of the same material, including the time-temperature shift factors for the two deformation modes in Section 4; we conclude with a summary.

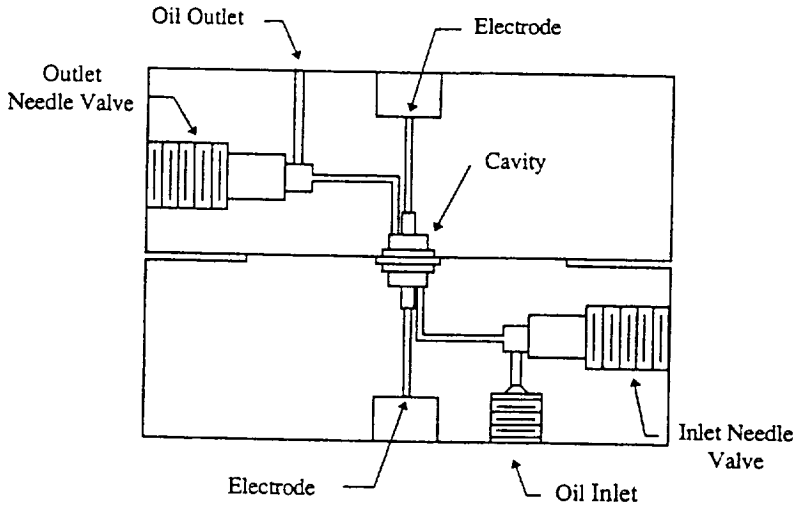

Figure 1. Pressure chamber.

2. Experimental Preliminaries

Among the several means possibly useful for the determination of viscoelastic bulk response, the method of determining the dynamic compliance with the aid of piezoelectric volume sensitive drivers and sensors appeared the most reliable. This method had been first demonstrated by McKinney et al. (1956), and employs a small cavity in a (nearly) rigid solid containing the polymer specimen and a non-conductive fluid. Two piezoelectric elements are housed in the cavity, of which one serves as a volume expander and the other as a pressure sensor. A sinusoidal voltage applied to one transducer causes expansion and contraction and thus pressure variations which then interact with the second piezoelectric element (pressure sensor). In this section we present the design and operation of the apparatus.

2.1. Pressure Chamber

The pressure chamber, shown in Figure 1, is constructed in two cylindrical halves of 303 stainless steel.[1] The nearly identical top and bottom are each 12.7 cm in outer diameter and 4.5 cm high. The mating surfaces are lapped and polished to ensure tight closure of the pressure chamber when the two halves are connected by six bolts (3/8" Allen screws). Needle valves are used in the inlet and outlet oil lines to minimize pressure variations generated in the chamber upon valve closure.[2]

Once the specimen is placed inside the 'lower' section of the chamber, the two halves are bolted together. Oil is pumped into the evacuated chamber[3] with a hand pump, until it exits through the top valve. The top valve (outlet) is closed first and the chamber is charged to the desired static pressure, then the bottom valve (inlet) is closed to isolate the chamber (pressure) from the supply and the environment. Prior

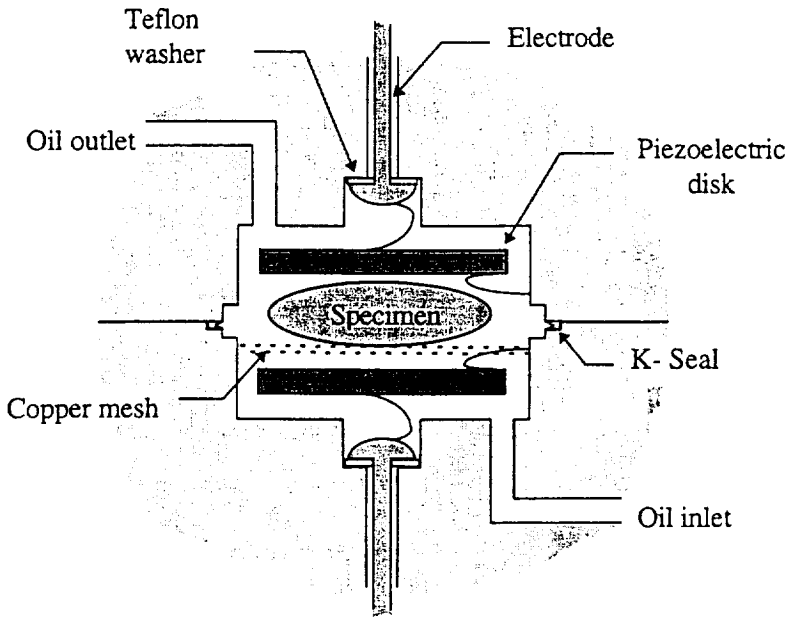

Figure 2. Cavity and piezoelectric transducers.

to charging the hand pump the pressure transmitting oil is degassed in a vacuum chamber until no bubbles can be detected. This oil degassing process requires about 24 hours for a liter of oil.

The cavity detail is sketched in Figure 2. The cylindrical cavity is 0.9 cm high by 1.0 cm in diameter. A copper mesh mounted in the bottom half of the pressure chamber supports the specimen. The chamber is sealed by means of a K-Seal which can be (re-)used with temperatures as high as 315°C and pressures of up to 410 MPa (70,000 psi).[4] Copper washers are used jointly with the K-Seal to obtain more consistent oil sealing. New copper washers are used each time the chamber is closed, so that a K-seal can be used repeatedly.[5] Since the sealing reliability depends on placing the components in nearly identical position relative to each other, alignment pins are used between the two chamber halves.

2.2. Piezoelectric Transducers and Electrical Feed-Through

The piezoelectric transducers are identical Lead Metaniobate disks 1.0 mm thick and 7.5 mm in diameter,[6] which are usable to temperatures of 300°C and pressures of up to 70 MPa. The flat surfaces of the transducer disks are silver coated for solder connections of copper leads. One face of each transducer disk is grounded to the pressure chamber through a mechanical pin connection while the other face is connected to respective electrodes via thin spiral copper wires.

An important detail in the operation is a trouble free electrical communication from the cavity to the measuring circuit. For working with elevated pressures

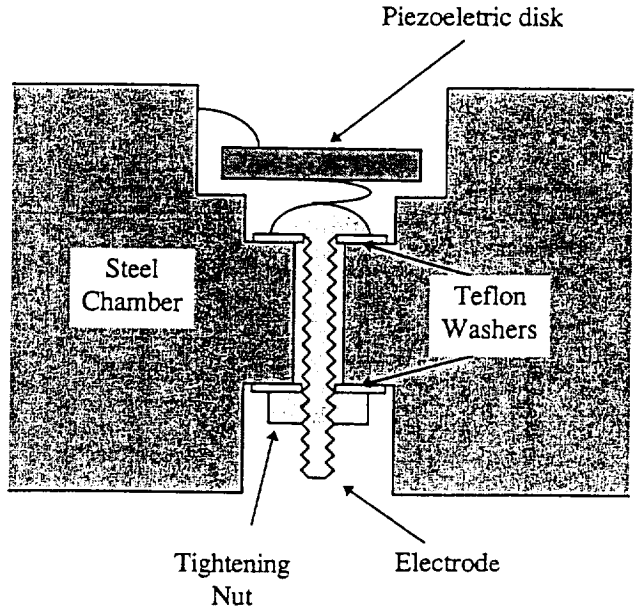

Figure 3. Electrode assembly.

the electrical connections must be passed pressure-tight through the cavity walls. Electrical connections[7] are made by passing the electrodes through the small holes (1.78 mm in diameter) in both halves of the pressure chamber. The assembly of the electrode is shown in Figure 3. The screw plugs function as both electrodes and sealing plugs for transmitting oil. The oil sealing and electricity insulation are achieved by using thin Teflon washers. The screws have to be tightened with sufficient force to form the oil seal but not too tightly so as not to damage the electrical insulation (Lin and Nolle, 1989). High temperature epoxy and ceramic bond adhesive were tried in the electrical connection but were unreliable because their coefficients of thermal expansion are substantially different from that of steel.

2.3. Measurement Circuitry

The schematic of the circuit for measuring the output of the piezoelectric disk is shown in Figure 4. A Stanford Research Systems (SRS) dual phase digital lock-in amplifier[8] (Model DSP SR830) and a charge amplifier are used to measure the voltage on the output piezoelectric transducer. The lock-in amplifier is capable of measuring the in-phase and out-of-phase signal relative to the reference signal with an accuracy of 0.001 mV. A function generator built into the SRS SR830 lock-in amplifier produces the sinusoidal voltage (5 V maximum) fed to the piezoelectric disk which serves as a volume expander. The reference frequency of the lock-in amplifier is set internally to the frequency of the signal generated by the function generator. In this way the noise level is reduced dramatically because the ampli-

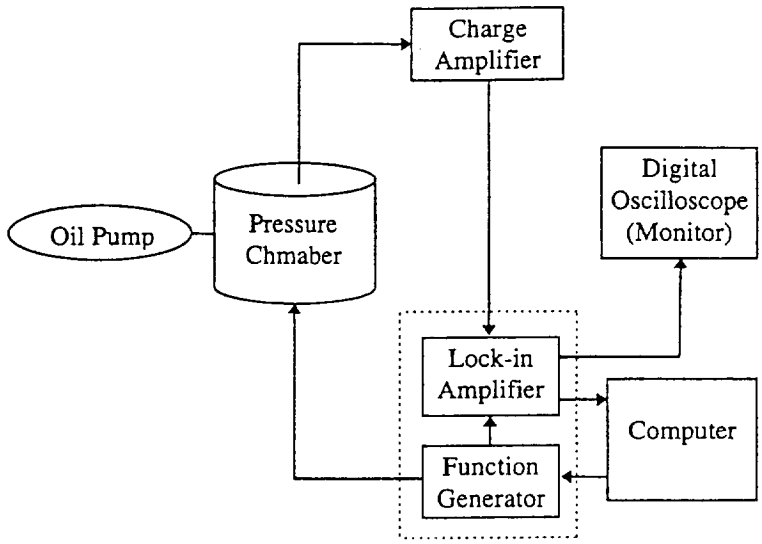

Figure 4. Experimental setup.

fier responds only to the frequency of the signal applied to the input transducer. Besides the high resolution of the lock-in amplifier its important contribution to the precision of the measurements is thus that they can all be made at very precisely predetermined frequencies and that interpolation between multiple measurements (calibration, see below) is obviated. The frequency as controlled by a digital SRS SR830 lock-in amplifier is accurate to 0.1 mHz. A digital oscilloscope (Nicolet Model 4049) monitors the output signal from the pickup transducer through the lock-in amplifier.

A piezoelectric transducer charge amplifier was built using a Bur-Brown OPA128 operational amplifier (cf. Figure 5) to possess a low cut-off frequency of 0.16 Hz. The OPA128 has excellent low-level signal handling capability and has a differential impedance of $10^{13}\Omega$. Because of this very high impedance, it becomes, however, the source of many kinds of noise, principally via electromagnetic interference from the input wires of the amplifier. All leads must thus be carefully shielded and grounded to reduce the noise level. The output from the pick-up piezoelectric transducer is less than 5 mV (RMS) for a 5 V (RMS) input to the driving transducer. Achieving a high electronic signal/noise ratio is, therefore, essential to obtain accurate bulk compliance measurements.

2.4. Thermal Control

The pressure cell is housed in a Grieve HT-800 industrial oven operating on a Honeywell (model UDC 3000) temperature controller. The temperature of the

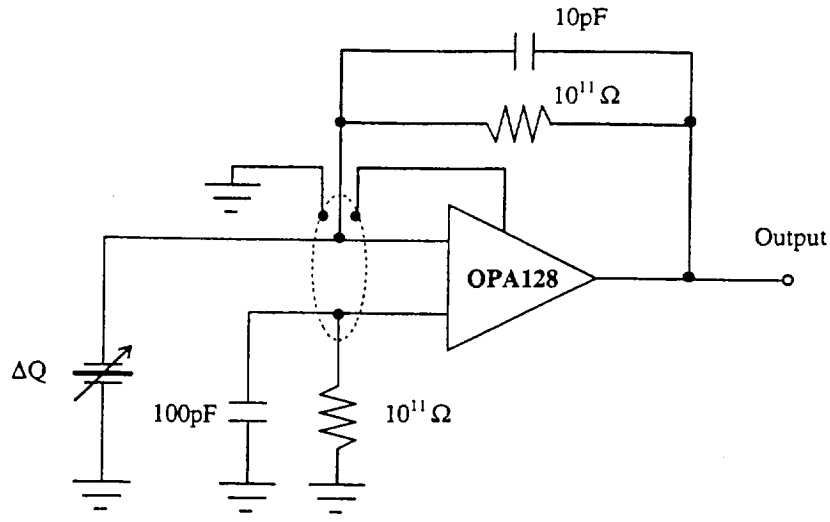

Figure 5. Piezoelectric transducer charge amplifier.

pressure chamber is monitored by nickel-iron thermocouples and temperature control is accurate to 0.1°C. The thermocouple leads are passed through the oil outlet to be as close to the cavity as possible; this thermocouple is withdrawn once the final temperature is reached and before measurements commenced. Because of the large thermal mass of the pressure cell typically three to four hours are required for the temperature to stabilize in the cavity. In order to prevent thermal pressure built up in the cavity, inlet and outlet oil ports are left open until the temperature has stabilized. As noted before, it requires several hours to stabilize the temperature inside the thick-walled pressure chamber, but once the desired temperature has been reached, it remains very constant because of the large thermal mass. Nevertheless, a time span of one to two hours is allowed to pass after withdrawal of the thermocouple in order to assure complete temperature stabilization.

2.5. The Frequency Range and Automation of the Experiment

There are two limitations to the useful frequency range: The upper frequency limit is governed by the size of the pressure cavity in that the dimensions of the specimen and of the cavity have to be small compared to the length of the pressure wave in the transmitting fluid; the lowest resonance occurs at 10 kHz. The lower frequency limit is imposed by the low frequency response of piezoelectric transducers which makes these devices virtually useless much below 1 Hz. Figure 6 shows the response of the apparatus (only oil in the cavity) over a large frequency range in which the response is most near to constant values in the range from 10 to 1,000 Hz – which was the range chosen for the subsequent measurements. For future operations expansion to three decades (3 to 3 kHz) is considered.

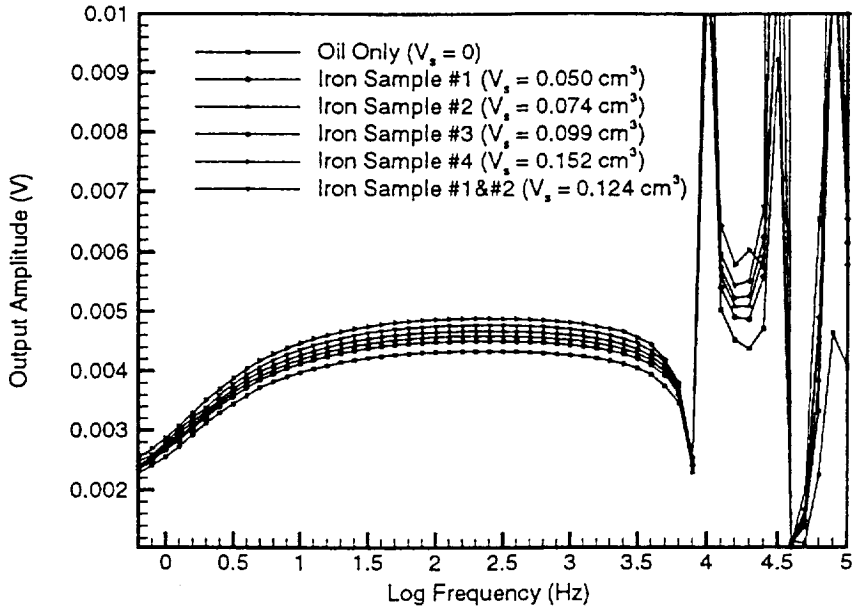

Figure 6. Output voltage on the pickup piezoelectric transducer in a wide frequency range (only oil in the cavity).

Under these conditions measurements can be considered as adiabatic. Marvin and McKinney (1965) deduced the 'critical' frequency for meeting adiabatic conditions of the sample as $f_c = \kappa/(C_p \rho x^2)$, where f_c is the critical frequency, C_p the specific heat at constant pressure, ρ the density of the sample, x the thickness of the specimen, κ the thermal conductivity of the polymer material. Based on this argument the critical frequency would be on the order of 0.01 Hz. At and above this frequency value there is insufficient time for appreciable heat conduction. Below this frequency measurements tend toward isothermal response.

The experiment is controlled by a computer (IBM 486DX2, 66 MHz) through serial communications with the SRS lock-in amplifier. The input voltage to the driving piezoelectric transducer is 5 V which is the maximum output from the built-in function generator. The computer sends out a command to set the frequency of the function generator, then waits for 30 seconds before it starts recording in-phase and out-of-phase voltages from the pick-up transducer. The voltages are sampled 30 times for 30 seconds, then averaged to reduce the random statistical error and stored on the hard disk. This procedure is repeated, computer controlled, over the frequency range of the experiment, for each temperature.

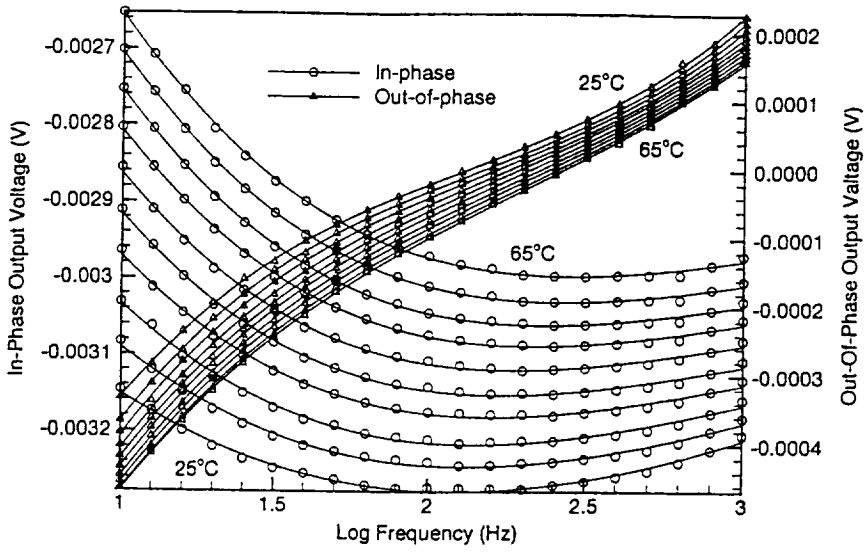

Figure 7. The in-phase and out-of-phase voltage output with oil only in the cavity, temperature ranges from 25 to 65°C in 5°C intervals.

3. Calibration

Because there are many parameters contributing to the final results which cannot be accounted for on the basis of 'first principles' the key to successful measurements is a careful calibration. The relation between the voltages of the piezoelectric disks is (McKinney et al., 1956).

$$\left(\frac{E_1}{E_2}\right)^* = A[C^* + (M_s^* - M_t)V_s],$$

where E_1 and E_2 are the complex (with time shift) voltages on the input and output piezoelectric transducers, M_s^*, M_t the complex bulk compliance of specimen and transmitting fluid, respectively, and V_s is the volume of the specimen. A and C^* are constants depending on the structure of the cavity, temperature, static pressure, frequency, and the subject of proper calibration.

The apparatus is calibrated using specimens of known properties, such as iron or magnesium, including calibration for the case when the chamber is filled with only the pressure transmitting fluid. Figure 7 shows the in-phase and out-of-phase output from the pick-up piezoelectric transducer with temperature from 25 to 65°C at atmospheric pressure. The in-phase voltage is negative because there is a 180° phase shift between the driving and pickup transducers as the result of the expansion of the driving transducer causing a compression on the pickup transducer. The absolute value of the in-phase voltage is on the order of millivolts while the out-of-

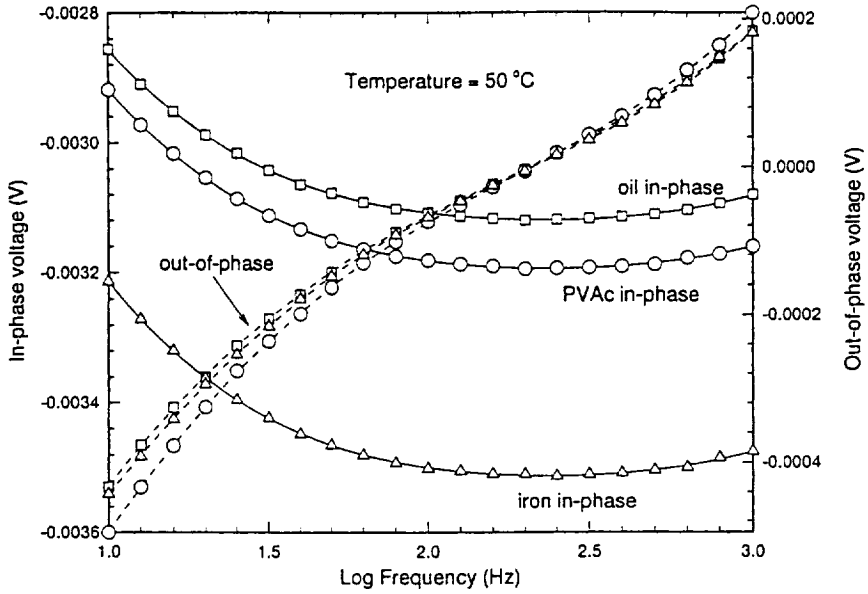

Figure 8. Example of in-phase (left ordinate) and out-of-phase (right ordinate) output voltages for oil plus iron and PVAc in the cavity at 50° C.

phase voltage is on the order of tenths of a millivolt. It is demonstrated in Figure 7 that a high accuracy of voltage measured on both in-phase and out-of-phase signals is achieved through the use of lock-in amplifier and the piezoelectric transducer charge amplifier.

The complex bulk compliance of PVAc was measured at frequencies from 10 to 1,000 Hz and at temperatures from 25 to 65°C in 5°C intervals. The calibrations of the pressure chamber to determine the two constants A and C^* were conducted on an oil-filled cavity (no specimen) and with an iron sample over the same range of frequencies and temperatures. We use the same oil as McKinney and Belcher (Di-2-ethylhexyl sebacate) so that the oil compressibility from that work is available. While we would expect purely elastic response of the system with oil and iron in the cavity, the detailed transducer response to sinusoidal excitation is not very well understood. The system requires then careful calibration over the whole range of frequency and temperature. The bulk compliance of iron is 0.587×10^{-11} m^2/N and independent of temperature in the range of these studies. The volume of the cavity in the pressure chamber is 0.785 cm^3. Iron disks having volumes of 0.096, 0.064, 0.048 and 0.032 cm^3 were used for calibration and the resulting measurements were then averaged to determine the constants. The input voltage is fixed at 5 V as generated by the built-in function generator of the lock-in amplifier.

An example of the in-phase and out-of-phase voltages from the output piezoelectric transducer is shown in Figure 8. Fourth order polynomial curve segments are fitted to the data to generate the smooth connections between data points. Measurements were actually carried out at frequencies from 2 to 5,000 Hz, but because of the poor responses at high and low frequencies only data between 10 and 1,000 Hz were processed.

4. Results and Discussion

In this section we report the detailed measurements and their evaluation relative to the bulk and shear response as measured by other investigators.

4.1. Specimen

The PVAc was purchased from Aldrich Chemical Company, and was nominally identical to the material used in earlier studies (Heymans, 1983), with an average molecular weight of the material of 16,700 and a density of 1.191 g/cm^3. The glass transition temperature as quoted by the manufacturer is 30°C which agrees closely with the value of 29.5°C determined by Heymans (1983). The PVAc comes in the form of irregular pellets ranging in weight from 0.1 to 0.3 gram. Each sample selected was microscopically examined to ascertain that they were void-free. The specimen volume was determined from the weight and the known specific volume of PVAc. The weight of the specimen pellets was checked repeatedly before and after the compliance measurements to detect any swelling or oil absorption. It was found that the weight of the pellets as measured by a digital balance with a precision of 1 mg (Mettler HL32) remained constant even after extensive exposure to the oil (at atmospheric pressure). The shape of the samples, however, changed during the sequence of measurements because tests were conducted well above the glass transition temperature so that the samples could deform under their own weight.

4.2. The Bulk Compliance

The storage and loss bulk compliances of PVAc at different temperatures and at the frequencies from 10 to 1,000 Hz are shown in Figure 9. The most pronounced change in the frequency dependent bulk compliance occurs at temperatures from 30 to 35°C. At lower temperatures (proximate bulk glassy state)[9] or higher temperatures (near-rubbery bulk state), the bulk compliance remains rather constant. Note that the loss compliance varies relatively little compared to the storage part, and resolution on the scale of the plot is poor. This variation becomes clearer in the following data analysis.

The data in Figure 9 are shown in Figure 10 shifted according to time-temperature superposition to produce the master curves; the storage and loss parts were shifted by the same amounts. The corresponding shift factors are shown in Figure 11. The storage and loss parts are, of course, not independent, so that the

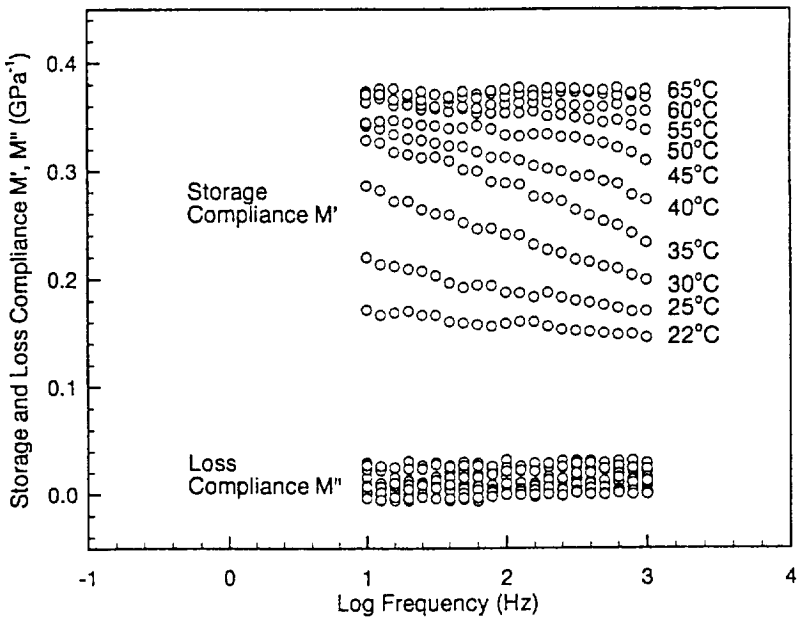

Figure 9. Storage $M'(f)$ and loss compliance $M''(f)$ of PVAc at indicated temperature over two decades of frequency.

loss part can be computed from the storage modulus (Ferry, 1980). Inasmuch as the former is so small and thus more subject to measurement errors, it is appropriate to examine its consistency in magnitude and frequency dependence with the storage modulus. Accordingly, the curve 'A' fitted to the storage compliance in Figure 10, is used to determine (numerically) the corresponding loss compliance, which is then shown as curve 'B' in the same figure. It is seen that the agreement is very satisfactory.

4.3. Comparison with Other PVAc Data

Having determined the bulk compliance over a significant time or frequency range it is of interest to compare this information with other data on PVAc, notably with the bulk data of McKinney and Belcher (1963), but also with time dependent shear behavior on the same material such as offered by Knauss and Kenner (1980), Heymans (1983), and Plazek (1980). Figure 12 shows the master curves for the storage and loss compliance of the McKinney and Belcher material along with the present data.[10] While the bulk measurements agree in the bulk rubbery domain, they differ in magnitude across the transition range, yielding a glassy-to-rubbery modulus ratio of about 2.8 for the present data as compared with a corresponding

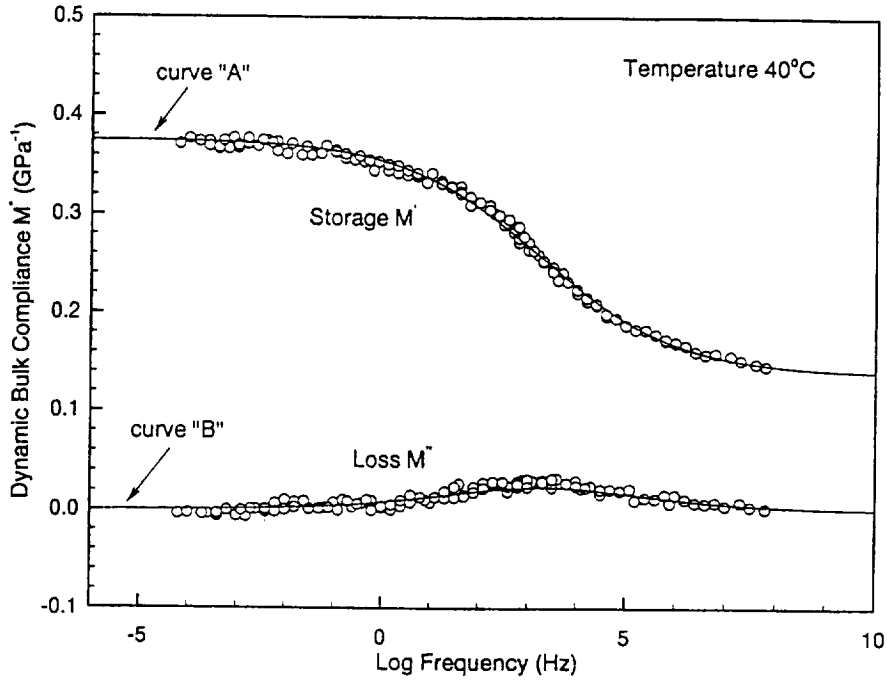

Figure 10. Master curve of storage and loss bulk compliance. Curve 'A', fitted to the storage compliance was used compute curve 'B' to represent the loss compliance.

value of 1.6 for the McKinney and Belcher data.[11] In addition, the frequency range across the transition is longer for the present data, being in excess of ten decades as compared to a range of about half that size for the McKinney and Belcher results.

It has often been argued that the transition of the bulk response should be shorter than that of the shear behavior, because the number of molecular deformation mechanisms contributing to bulk deformations should be markedly smaller than those that control shear behavior. With this idea in mind we show in Figure 13 the dynamic shear compliance for the same Aldrich material used in the bulk deformation studies as computed from Knauss and Kenner's data (1980) together with Heymans' (1983) and Plazek's (1980) results. We note that the transition ranges for the shear and for the bulk responses are comparable, seemingly contradicting the idea that bulk deformation involves fewer relaxation times than shear response.

More important, however, is the fact that the transition ranges for the two material functions do not overlap materially: The bulk response exhibits its transition behavior in essentially the glassy (high frequency) domain of the shear behavior, with the two transition ranges being separated by about ten to twelve decades.* This

* The precision of this statement suffers from the lack of a metric for the definition of the 'width of the transition range'.

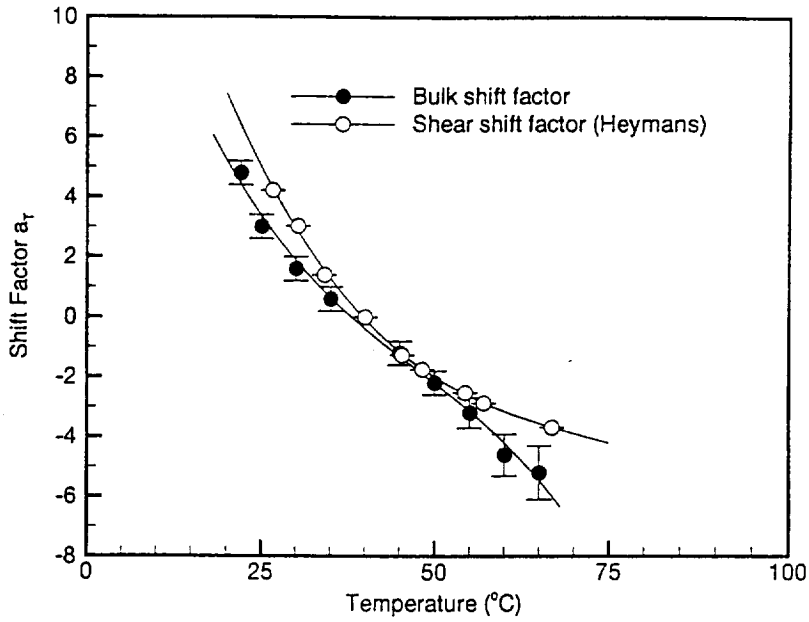

Figure 11. Bulk compliance shift factor comparison with shear modulus shift factor (Heymans, 1982).

significant difference in the mean time of the transition ranges of the two material functions indicates that the molecular contributions to these two types of deformations mechanisms derive from different chain and/or side-group mobilities. This observation for the (very) small deformation behavior (linearly viscoelastic range) is at variance with the response at moderate but non-infinitesimal deformations for which there exists a distinct interaction between shear and dilatational stress and deformation states in determining the time dependent material response (Lu and Knauss, 1997).

The difference in molecular deformation sources is also apparent in the comparison of the shift-factors as derived from the bulk data with those obtained from the shear data. In Figure 11 the solid data points represent the shift factors derived in forming the bulk compliance master curves in Figure 10, while the open symbols represent the shift data derived in producing the shear modulus data in Figure 13. Inasmuch as the temperatures are principally above the glass transition the WLF response appears appropriate for the shear data. On the other hand, the bulk response elicits a shift behavior that is much more akin to Arrhenius behavior with a more linear relation than the WLF equation would represent.

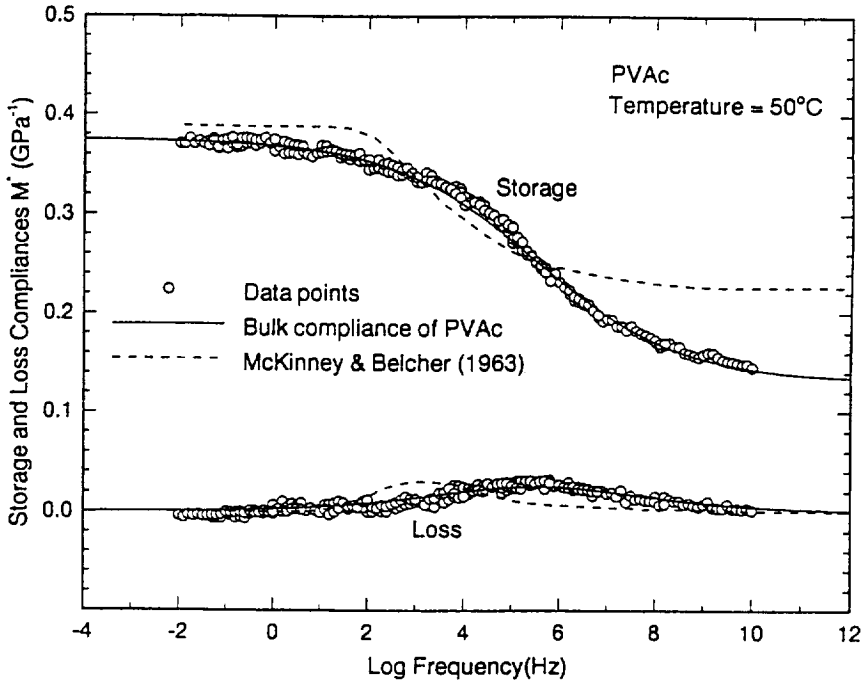

Figure 12. PVAc bulk compliance; comparison with McKinney and Belcher data.

5. Concluding Remarks

We have confirmed that the viscoelastic bulk response of PVAc under near-infinitesimal deformations possesses a transition range separating its 'glassy' and 'rubbery' responses. Although different versions of the same chemical material have been studied in the past similar results obtain in that the ratio of the short-term to long-term response is about 2.8 as compared with a value of 2.6 for a material of similar molecular weight (Lin and Nolle, 1989) and 1.6 for the studies of McKinney and Belcher (1963) on a PVAc material not described any closer. This bulk response spectrum falls in essentially the time or frequency domain associated with the 'glassy' shear response for this material. Apart from this mismatch the transition domains extend over roughly comparable time decades; this latter result is at variance with the findings of McKinney and Belcher on a seemingly different PVAc material.

The present results confirm thus that time or rate dependent deformations derive from different sources at the molecular level, which observation speaks for the mutual independence of the shear and bulk properties at infinitesimal deformations which underlie the linearized theory of viscoelasticity. Based on parallel experimental studies, this independence appears to cease once larger than truly small

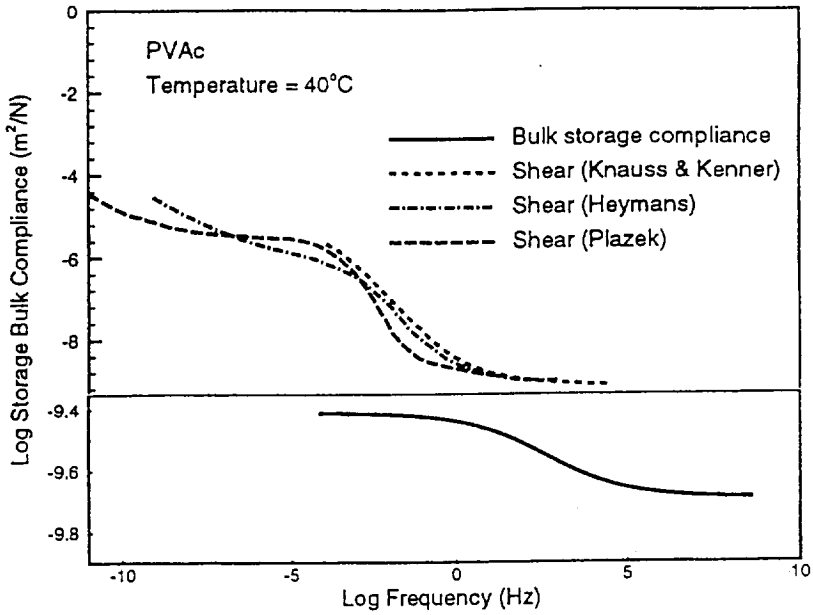

Figure 13. Comparison of shear and bulk compliances for PVAc. Knauss and Kenner, Heymans data for same molecular weight PVAc (167,000) as for present study. Plazek's high molecular weight material has Mw = 650,000.

deformations are involved, a first estimate for the boundary being projected for strains on the order of about 0.2%.

Acknowledgements

This work was initially supported by ONR grant N00014-91-J-1427 with Dr. Peter Schmidt as the monitor, and later work was supported by NASA under grant #NSG 1483 and #NAG 1-1780, with Dr. Tom Gates as the technical monitor. In addition funds from the National Science Foundation under grant #CMS9504144 allowed completion of this study.

Notes

[1] We are indebted to C. Schultheisz for the initial design of this part of the apparatus.

[2] Valves and oil fittings were purchased from High Pressure Equipment Company, Erie, PA.

[3] Evacuation before and during the oil-filling procedure to eliminate trapped air in the chamber.

[4] At this time no measurements at elevated pressures have been made, though they are intended later. Also, the apparatus has been designed to accommodate materials with higher glass transition temperatures.

[5] Each compression of the K-seal causes a tiny compression set; this cumulative effect is alleviated through the use of fresh copper washers. The K-seals were designed and manufactured by Sierracin/Harrison Corporation, Burbank, CA.

[6] The Lead Metaniobate disks were purchased from Piezo Kinetics Inc., Bellefonte, PA.

[7] Shielded BNC connectors and shielded cables are essential to reduce noise on both piezoelectric transducers.

[8] A lock-in amplifier has the ability to measure the signal in a very narrow frequency band-width so that it targets the signal measurement at a specific frequency.

[9] The current equipment does not allow for reliable temperature control below room temperature. Thus the lowest temperature recorded is 22°C.

[10] The data for the references by Heymans and Knauss and Kenner are in terms of creep compliance. For the present purposes it is deemed sufficient to have the storage compliance reproduced by replacing t by $1/f$ in the creep compliance. The time or frequency range of concern here is much larger than the error incurred in this simplification.

[11] The corresponding range for medium molecular weight PVAc as measured by Lin and Nolle (1989) appears to be about 2.6.

References

Duran, R.S. and McKenna, G.B., 'A torsional dilatometer for volume change measurements on deformed glasses: Instrument description and measurements on equilibrated glasses', *J. Rheology* **34**, 1990, 813.

Ferry, J.D., *Viscoelastic Properties of Polymers*, 3rd Edition, Wiley, New York, 1980.

Heydemann, P., 'The dynamic compressibility of high polymers in the frequency range from 0.1 c/s to 60 kc/s', *Acustica* **9**, 1959, 446.

Heymans, L.J., 'An engineering analysis of polymer film adhesion to rigid substrates', Ph.D. thesis, California Institute of Technology, 1983.

Knauss, W.G. and Emri, I.J., 'Non-linear viscoelasticity based on free volume consideration', *Computers and Structures* **13**, 1981, 123.

Knauss, W.G. and Emri, I.J., 'Volume change and the non-linearly thermo-viscoelastic constitution of polymers', *Polymer Engineering and Science* **27**, 1987, 86.

Knauss W.G. and Kenner, V.H., 'On the hygrothermomechanical characterization of polyvinyl acetate', *J. Appl. Phys.* **51**, 1980, 5131.

Lin, T.S. and Nolle, A.W., 'Dynamic compressibility of poly(vinyl acetate) and poly(methyl methacrylate): Effects of molecular weight', *Polymer* **30**, 1989, 648.

Losi, G.U. and Knauss, W.G., 'Free volume theory and nonlinear thermoviscoelasticity', *Polymer Science and Engineering* **32**, 1992, 542.

Lu, H. and Knauss, W.G., 'Non-linear viscoelastic behavior of PMMA under multiaxial stress states', GALCIT SM Report 96-6, *Mech. Time-Dep. Mat.* **1**, 1997 (to appear).

Marvin, R.S. and McKinney, J.E., 'Volume relaxation in amorphous polymers, physical ccoustics', *Physical Acoustics* Vol. IIB, W.P. Mason (ed.), Academic Press, New York, 1965, 165.

McKinney, J.E. and Belcher, H.V., 'Dynamic compressibility of poly(vinyl acetate) and its relation to free volume', *J. Research of National Bureau of Standards, A. Physics and Chemistry* **67A**, 1963, 43.

McKinney, J.E., Edelman, S., and Marvin, R.S., 'Apparatus for the direct determination of the dynamic bulk modulus', *J. Appl. Phys.* **27**, 1956, 425.

Plazek, D.J., 'The temperature dependence of the viscoelastic behavior of poly(vinyl acetate)', *Polymer Journal* **12**, 1980, 43.